INTERNATIONAL UNION FOR QUATERNARY RESEARCH

International Inter-INQUA Field Conference and Workshop on Tephrochronology, Loess, and Paleopedology

University of Waikato, Hamilton, New Zealand
7-12 February, 1994

INTRA-CONFERENCE AND POST-CONFERENCE TOUR GUIDES

Edited by

D. J. Lowe

Department of Earth Sciences, University of Waikato, Private Bag 3105,
Hamilton, New Zealand

Bibliographic citation for entire guidebook:

Lowe, D.J. (editor) 1994. Conference Tour Guides. *International Inter-INQUA Field Conference and Workshop on Tephrochronology, Loess, and Paleopedology,* University of Waikato, Hamilton, New Zealand. 186p.

Bibliographic citation for sections within the guidebook (e.g.):

Pillans, B.J.; Palmer, A.S. 1994. Post-Conference Tour Day 3: Tokaanu—Wanganui. *In* Lowe, D.J. (ed) Conference Tour Guides. *International Inter-INQUA Field Conference and Workshop on Tephrochronology, Loess, and Paleopedology*, University of Waikato, Hamilton, New Zealand: 139-156.

Acknowledgements

I thank all the contributors to the guide for their written efforts, and for fine leadership in the field. Ian Nairn (IGNS) is especially thanked for co-leading part of Day 2 of the Intra-Conference Field Trip, and Neill Kennedy (formerly DSIR), Dennis Eden (Landcare Research), and Ron Kimber (CSIRO) are thanked for providing unpublished information. I have appreciated special assistance from Laurence Gaylor (field site preparation), Mike Green (back-up vehicle), Frank Bailey (drafting), Cam Nelson (departmental support) (all University of Waikato), and Carole Mardon and other staff of the University of Waikato Printery. The various people or organisations who hosted or transported the tour parties, or willingly allowed access to private land, are also thanked.

D.J. Lowe (Editor)

Note: Throughout the text, Ma = millions of years before present, ka = thousands of years before present.

DAY 2: HAMILTON—ROTORUA—HAMILTON

Lowe, D.J.; Briggs, R.M. 1994. Intra-conference Tour Day 2: Hamilton–Rotorua–Hamilton. In: Lowe, D.J. (ed) Conference Tour Guides, Proceedings International Inter-INQUA Field Conference and Workshop on Tephrochronology, Loess, and Paleopedology, University of Waikato, Hamilton, New Zealand, 45-71.

D. J. Lowe & R. M. Briggs
Department of Earth Sciences
University of Waikato, Private Bag 3105
Hamilton, New Zealand

Outline of Day 2 (Thurdsay 10 February)

8.30-9.10 am	Depart Bryant Hall, University of Waikato, and travel (SH 1) to Hinuera Quarry
9.10-9.50 am	STOP 1 — Ongatiti Ignimbrite, Hinuera Quarry
9.50-10.05 am	Travel to Tirau
10.05-10.15 am	STOP 2 — Comfort stop, Tirau
10.15-10.30 am	Travel from Tirau to Tapapa
10.30-11.15 am	STOP 3 — Tapapa Section, Tapapa
11.15-12.00 pm	Travel to Rainbow Springs, Rotorua
12.00-1.30 pm	STOP 4 — Rainbow Springs LUNCH at Springs Restaurant 12.00-12.45 pm Tour of Springs 12.45-1.30 pm
1.30-2.00 pm	Travel to Te Ngae
2.00-2.45 pm	STOP 5 — Te Ngae Section, Te Ngae
2.45-3.00 pm	Travel to Gisborne Point (Lake Rotoiti) and enter Rotoiti Forest on Rotoiti Rd
3.10-5.00 pm	STOPS 6, 7, & 8 — Three sections on Rotoiti Rd of proximal Holocene eruptives, Haroharo Caldera
5.00-6.00 pm	Travel from Haroharo Caldera to Aorangi Peak Restaurant, Mt Ngongataha (Rotorua)
6.00-6.30 pm	STOP 9 — Overview of Rotorua Caldera and Okataina Volcanic Centre, from Aorangi Peak Restaurant
6.30-8.30 pm	CALDERA DINNER at Aorangi Peak Restaurant (Tarawera Room)
8.30-10.00 pm	Return from Rotorua to Bryant Hall, University of Waikato, Hamilton

INTRODUCTION

We have a reasonably long day ahead of us, but it promises to be both interesting and relaxing. We will be examining a range of distal and proximal pyroclastic deposits including airfall and flow (ignimbrite) units derived from the Mangakino and Okataina Volcanic Centres, Taupo Volcanic Zone (TVZ), tephric loess deposits, and buried paleosols on tephra beds — in other words, something for everyone attending our three-discipline conference. As well, we shall see a variety of volcanic landforms both on our journey from Hamilton and in the Rotorua region itself. We finish the day with a 'Caldera Dinner' overlooking Rotorua and Haroharo calderas, and Mt Tarawera, from the top of Ngongataha rhyolite dome.

From Hamilton (Fig. 2.1) we initially travel SE over the surface of a large, low angle fan of volcaniclastic sediments (the Hinuera Formation) deposited by an ancestral Waikato River system (Hume et al. 1975; Green & Lowe 1985; Selby & Lowe 1992). The age of this surface in the Hamilton Basin is c. 18-15 ka, and is mantled with a thin cover of distal tephra beds from various sources (Lowe 1986, 1988).

Stop 1 (off SH 29) is located in a quarry on cliffed margins in a shallow valley running approximatey N-S. The valley was previously occupied by the Waikato River discharging into the Hauraki Gulf/Firth of Thames (between c. 0.14 Ma and 50 ka, and between c. 24-19 ka; Selby & Lowe 1992).

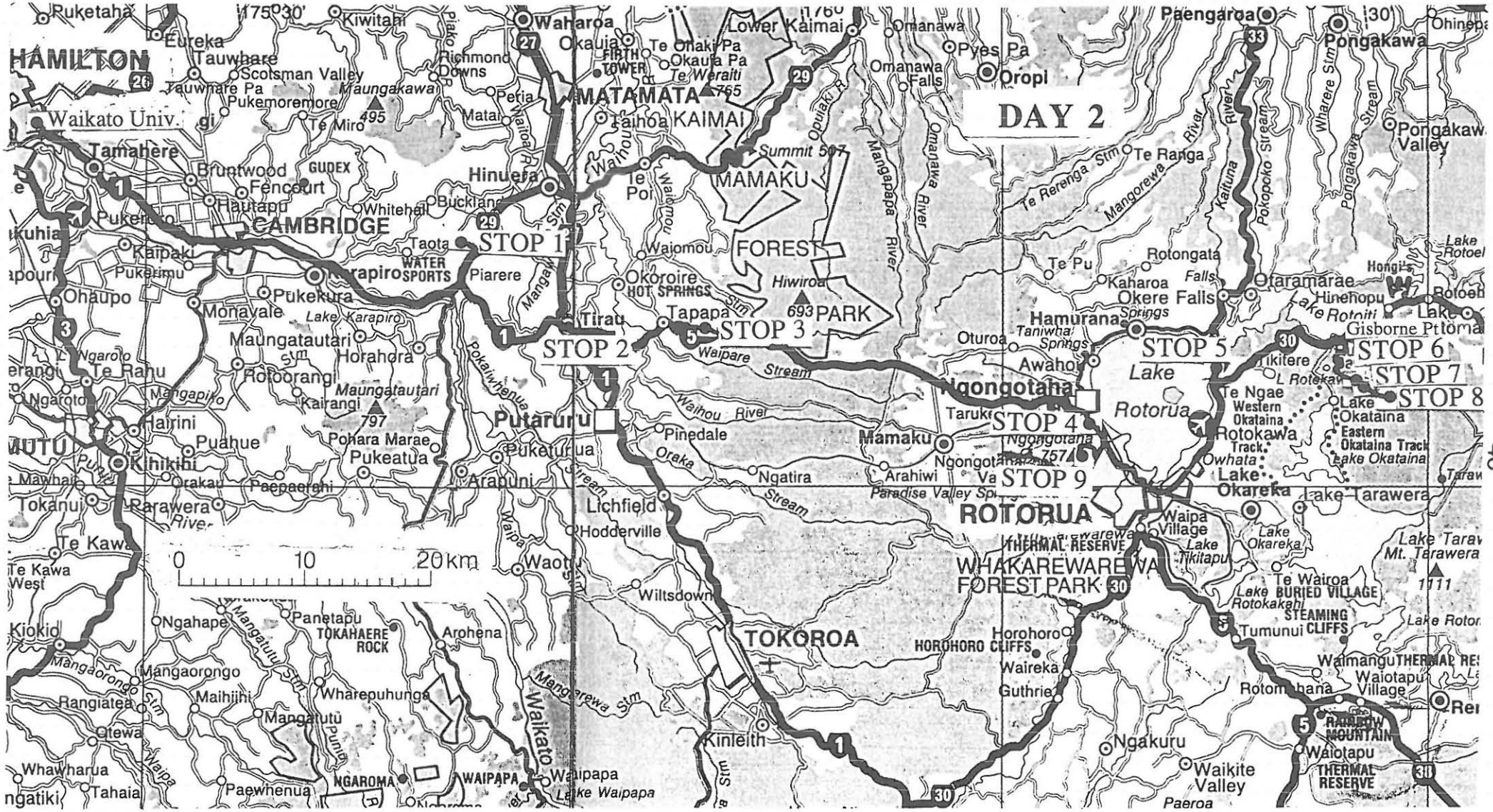

Figure 2.1: Route map for Day 2.

STOP 1 — Ongatiti Ignimbrite, Hinuera Quarry (T15/461614)
[Note: Hard hats must be worn]

The quarry (owned by Firth Industries) is developed in cliffs of Ongatiti Ignimbrite. The ignimbrite here is overlain by a 5+ m thick sequence of tephra beds including Hamilton Ash and younger airfall tephras.

TABLE 2.1. Summary of the stratigraphy, age, and characteristics of eruptives from the Mangakino Volcanic Centre (from Briggs et al. 1993).

Name	Ar/Ar age (Ma)	Volume (km^3)	Composition (SiO_2 wt.%)	Aspect ratio*	Nature
Waioraka Ignimbrite	–	<0.1	–	–	Non-welded, pumice-rich, vapour-phase altered ignimbrite with abundant lithic-rich lenses.
Whakaahu lava dome	0.87±0.08	<1	–	–	
Marshall Ignimbrites	0.91±0.02	>50	71–77	1:700	Marshall A: partially to densely welded ignimbrite, brown pumice, crystal-rich, pale buff-brown matrix. Marshall B: non-welded to partially welded, crystal-poor ignimbrite, with black and orange-brown pumice in a sandy black matrix. (Marshall A and B correlated with Ignimbrite I of Wilson, 1986).
Kaahu Ignimbrite	0.92±0.07	<0.5	74	–	Pumice-rich, crystal-poor ignimbrite, extensively vapour-phase altered. (Correlated with Ignimbrite H of Wilson, 1986).
Rocky Hill Ignimbrite	0.97±0.02	>300	71–76	1:3,200	Partially to densely welded, pumice-rich, crystal-rich ignimbrite with abundant hornblende.
Unit E	1.01±0.06	>300	71–76	–	Poorly exposed phreatomagmatic fall deposits with overlying non-welded ignimbrite.
Ahuroa Ignimbrite	1.19±0.03	>50	65–76	1:6,000	Non-welded to densely welded ignimbrite with an inverse thermal zonation; lower unit is crystal-rich with orange platy rhyolitic pumice and black dacitic pumice in a sandy black matrix, upper unit is strongly lenticular with fiamme.
Unit D	1.18±0.02	>10	67–75	–	Phreatomagmatic fall deposits with overlying non-welded ignimbrite.
Ongatiti Ignimbrite	1.23±0.02	>300	70–75	1:4,000	Pumice-rich, crystal-rich, non-welded to partially non-welded ignimbrite.
Tumai lava dome	1.27±0.05	<0.1	–	–	
Ignimbrite C	1.62±0.11	>10	60	–	Poorly exposed, partially welded andesitic ignimbrite.
Ignimbrite B	1.51±0.02	?	–	–	Poorly exposed, partially welded ignimbrite, extensively vapour-phase altered.
Ngaroma Ignimbrite	1.60±0.03	>50	71	1:3,000	Partially welded, purplish-brown extensively vapour-phase altered ignimbrite. (Correlated with Ignimbrite A of Wilson, 1986).

*Aspect ratio is defined by Walker et al. (1980) and Walker (1983) as V/H, where V is the average thickness, and H is the diameter of a circle covering the same areal extent as the rock unit.

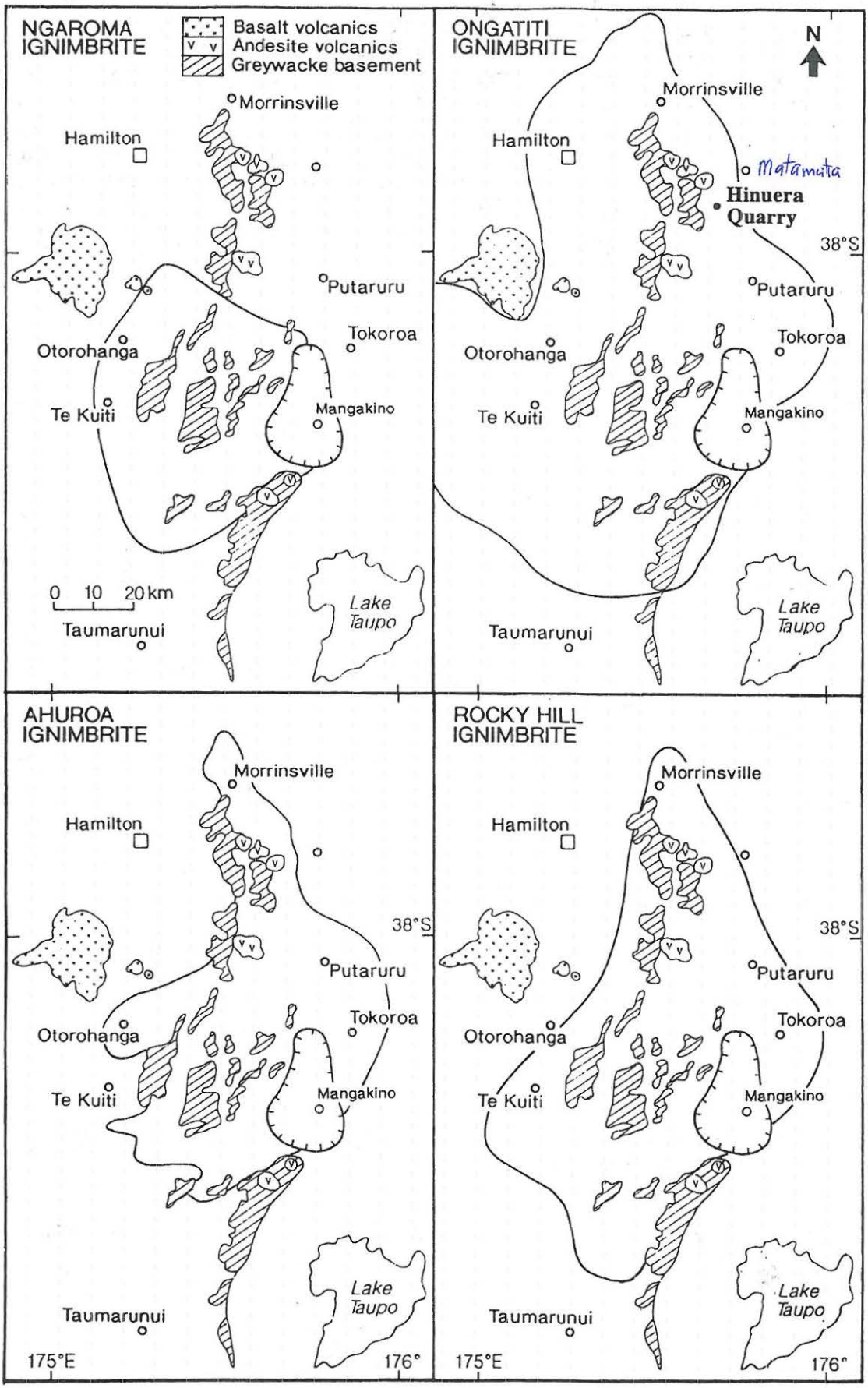

Figure 2.2: Distribution of four major Mangakino-derived ignimbrites, including Ongatiti. Lines represent envelopes around the outermost preserved outcrops and exposures, which are mainly the partially and densely welded portions of the units; hence they represent minmal areas covered by the deposits because of erosion, and the original nonwelded portions were much more widespread (from Briggs et al. 1993). The delineation of the Mangakino caldera is after Wilson et al. (1984).

The Ongatiti Ignimbrite, dated at 1.23 ± 0.02 Ma, is one of at least three ignimbrites derived from Mangakino volcano mapped in this area (Fig.2.2), the others including Ahuroa (1.19 ± 0.03 Ma) and Rocky Hill (0.97 ± 0.02 Ma) ignimbrites that lie above Ongatiti (Table 2.1; Briggs et al. 1993). In this section, the Ongatiti Ignimbrite has prominent but widely-spaced columnar jointing. It comprises a lower pumice-poor, crystal-rich, lithic-poor unit, a middle moderately welded flow unit, and an upper pumice-rich partially welded* unit (Fig. 2.3). The upward coarsening and abundance of pumice is also matched by the lithics, and so is not simply a fluidization-induced grading. These stratigraphic relations imply that the the ignimbrite consists of multiple flows that were erupted in a series of directional lobes. Briggs et al. (1993) suggested that the Ongatiti eruption commenced with highly energetic, violent and relatively cool flows which generated the finer-grained lower pumice-poor flows, and the eruption later escalated into a series of hotter but less energetic, coarser-grained pumice flows.

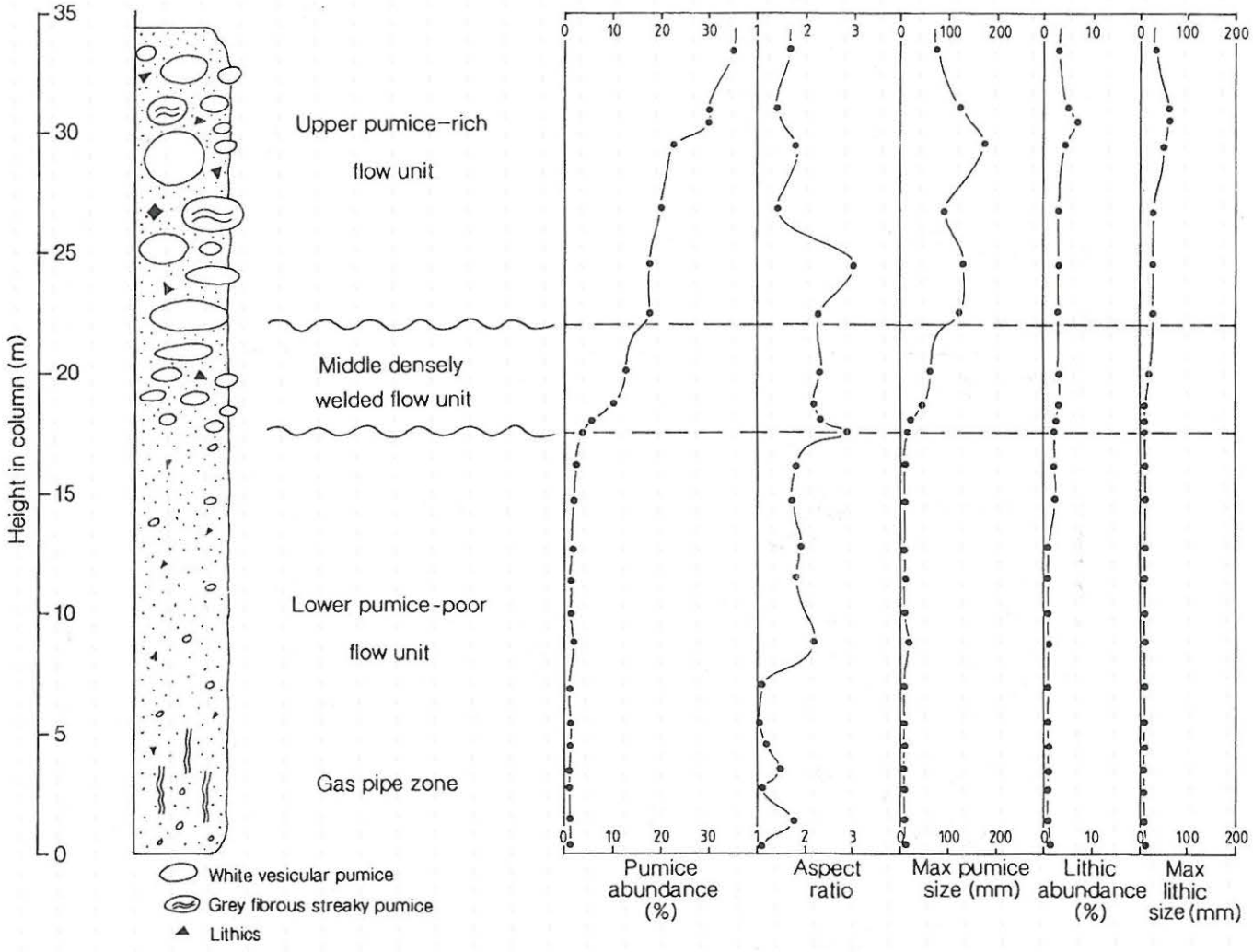

Figure 2.3: Stratigraphic section of Ongatiti Ignimbrite at Hinuera Quarry (from Briggs et al. 1993).

lithics - incl. rhyolite microdiorite gneiss

* Note: Ignimbrite welding (the sintering together of hot pumice fragments and glass shards under a compactional load; Cas & Wright 1987) can be described on a four-point scale: non-welded (can pluck pumicefragments out by hand) — weakly welded — partially welded — densely welded (pumice clasts break when ignimbrite cracked with hammer).

Mineralogically, plagioclase (oligoclase, andesine) is the dominant crystal and phenocryst, together with quartz, orthopyroxene (mainly ferrohypersthene), calcic hornblende, titanomagnetite, ilmenite, zircon, and apatite (Briggs et al. 1983). Glass shard analyses show a noteably homogenous composition (Table 2.2), and hence provide little evidence for mixing, whereas analyses of whole pumice clasts (i.e. glass in pumice + phenocrysts) are heterogeneous and, in contrast, provide evidence for mixing (Briggs et al. 1993). Other major- and trace-element analyses show that pumice in Ongatiti Ignimbrite varies compositionally (from 69.7 to 73.5 wt% SiO_2) but there are no systematic trends with stratigraphic height in the ignimbrite. Rather, pumices adjacent to one another in outcrop have variable composition, and the lack of any systematic trend is consistent for all oxides and trace elements. The compositional variation in pumice fragments demonstrates that the magma chamber was not homogenous but contained a significant range of compositions.

TABLE 2.2. Representative microprobe glass shard compositions in the Ongatiti Ignimbrite, normalised to 100% water free (from Briggs et al. 1993).

Sample	0/18	0/18	0/12	0/12	0/10	0/10	0/17	0/17	0/21	0/20
SiO_2	76.95	77.50	77.51	77.58	77.49	77.39	77.88	76.85	77.08	77.30
TiO_2	0.12	0.12	0.13	0.10	0.13	0.14	0.10	0.17	0.12	0.19
Al_2O_3	12.69	12.40	12.44	12.33	12.29	12.18	12.19	12.70	12.41	12.46
FeO*	1.14	1.42	1.07	1.25	1.32	1.43	1.15	1.21	1.36	1.36
MnO	–	–	–	–	–	–	–	–	–	–
MgO	0.11	0.11	0.07	0.06	0.12	0.08	0.12	0.12	0.11	0.09
CaO	0.87	0.82	0.66	0.77	0.74	0.82	0.61	0.73	0.53	0.86
Na_2O	3.52	3.47	3.32	3.21	3.33	3.33	3.31	3.44	2.47	3.23
K_2O	4.34	3.90	4.46	4.48	4.26	4.36	4.35	4.52	5.60	4.34
Cl	0.26	0.26	0.34	0.22	0.32	0.27	0.29	0.26	0.32	0.17

* Total Fe

Briggs et al. (1993) additionally report REE and Sr and Nd isotope analyses for Ongatiti Ignimbrite, and discuss these with respect to parallel analyses on other Mangakino eruptives and their petrogenesis.

Quarrying operation

The Ongatiti Ignimbrite, known commercially as Hinuera Stone (Hinuera locality is nearby), was first quarried experimentally in 1894 for corners and window surrounds of 'Bishop's Palace' in Ponsonby, Auckland; these are still in good condition. Although the Government Geologist, P. Marshall, suggested in 1923 that Hinuera Stone would be suitable for building purposes (and several houses were built using it in the mid 1930s), it was only in 1954 that the present quarry commenced full commercial operations. This took place because of the development of new techniques in quarrying that reduced costs significantly. The ignimbrite is cut into blocks of various sizes and widely used thoughout the North Island, mostly as a cladding stone for quality houses or decorative stone walls (Hayward 1987). Sometimes the faces of ignimbrite slabs have been heated with oxy-acteylene torches which vitrify the natural glass and result in a sparkling glass surface, occasionally coloured as well, and useful as facing panels in murals. The blocks are extracted using a combination of explosives, giant chain saws, and large air bags to 'lift' blocks from the outcrop face.

STOP 3 — Tapapa Section, Tapapa (T15/635524)

At this site the main focus is on the cover bed stratigraphy, but we will also be able to look at Mamaku Ignimbrite and a classic Andisol. In addition, there are good views from the top of the section of the interfluve surfaces with patches of indigenous forest and, to the N, the low-lying Hauraki Depression, a large continental rift structure (Hochstein & Nixon 1979; Hochstein et al. 1986; de Lange & Lowe 1990).

Andesitic volcanic centres of late Miocene age, the Kiwitahi Volcanics, extend along the western boundary of the Hauraki Rift (Black et al. 1992); Maungatautari volcano, an isolated, bush-covered andesite-dacite composite volcano dated at 1.8 Ma (Briggs 1986), lies to the SW .

The Tapapa Section, on private land owned by B. and J. Goodwin, lies at an elevation of ≈260 m, has an annual rainfall of 1600 mm, and a mean annual temperature of ≈13°C. Native vegetation since c. 15 ka was almost certainly mixed broadleaf-podocarp forest (Newnham et al. 1989). The modern soils (Waiohotu series) are Typic Hapludands (McLeod 1992) (see Table 2.6). The 7 m section exposed here contains a comprehensive stratigraphic record of tephra deposits, tephric loess, and buried paleosols representing alternating periods of deposition and soil formation over the past c. 140 ka on the Mamaku Plateau (Kennedy 1982, 1988, in press). The section is described in Table 2.3 and the stratigraphy summarised in Fig. 2.4.

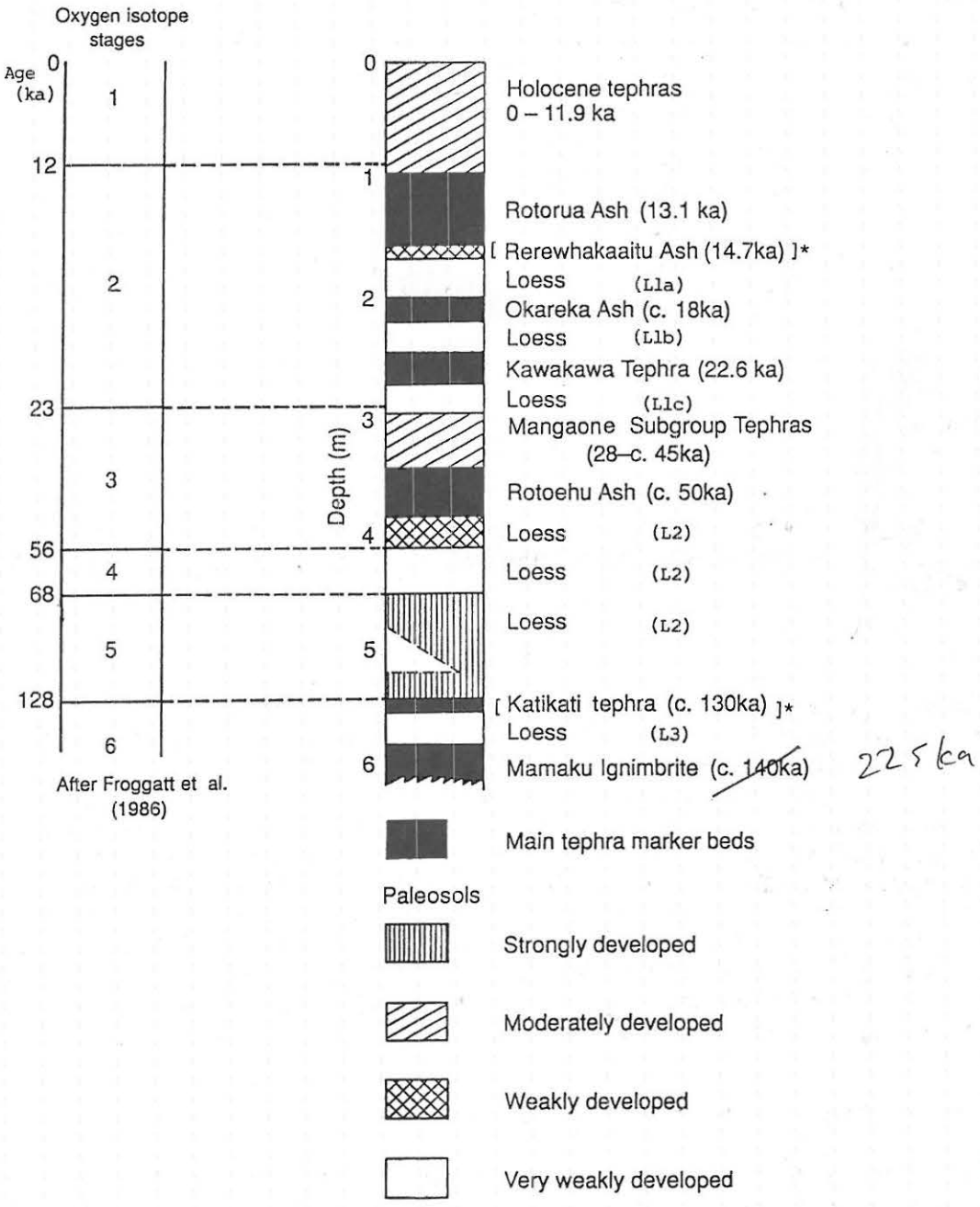

Figure 2.4: Stratigraphy of cover beds on the Mamaku Plateau and correlation with the marine oxygen isotope record (from Kennedy in press). The Tapapa section, on which the diagram is based, provides the best stratigraphic record of the cover bed stratigraphy. * Not present at Tapapa. Loess units from Eden et al. in prep.).

TABLE 2. 3. Description of Tapapa section (from Kimber et al. in press).

Depth (m)	Description	
0.00 - 1.00	Multiple Holocene tephra deposits (not differentiated): dark yellowish brown (10YR 5/6) to yellowish brown silt loam; moderately weak; weakly developed nut and block structure; indistinct boundary,	Waiohotu gritty silt loam
1.00 - 1.15	Rotorua Tephra (c.13.4 ka): brownish yellow (10YR 6/6) coarse sand; moderately weak; massive breaking to single grain structure; indistinct boundary,	Rr
1.15 - 1.45	Loess: yellowish brown (10YR 5/4) silt loam; moderately firm; weakly developed coarse blocky structure; distinct boundary,	Loess 1a*
1.45 - 1.60	Okareka Tephra (c.18 ka): yellowish brown (10YR 5/6) sandy loam; moderately firm; massive structure; distinct boundary,	Ok
1.60 - 2.00	Loess: yellowish brown (10YR 5/4) silt loam; moderately firm; massive structure; distinct boundary,	Loess 1b
2.00 - 2.45	Kawakawa Tephra (c. 22.5 ka): very pale brown (10YR 7/3) and pink banded silt loam, and sandy loam; moderately firm; massive structure; sharp boundary,	Kk
2.45 - 2.65	Loess: light yellowish brown (10YR 6/6) silt loam; moderately firm; massive structure; few Fe/Mn concretions; indistinct boundary,	Loess 1c
2.65 - 3.35	Palaeosol (in tephra): yellowish brown (10YR 5/6) gritty silt loam; moderately firm; weakly developed coarse blocky structure; horizon includes some Mangaone Subgroup tephras (c. 28-45 ka); indistinct boundary,	Pal 2a
3.50 - 3.95	Rotoehu Ash (c. 50 ka): light grey, yellow and very pale brown layered loamy sand to silt loam; moderately firm to very firm; massive structure; indistinct boundary,	Re
3.95 - 4.20	Weak palaeosol (in loess): brown (10YR 5/3) silty clay loam; moderately firm; massive structure; indistinct boundary,	Pal 2b
4.20 - 4.73	Loess: yellowish brown (10YR 5/4) silty clay loam; moderately firm; massive structure; indistinct boundary,	Loess 2
4.73 - 5.63	Strong palaeosol (in loess but includes some andesitic tephra deposits): dark yellowish brown (10YR 4/4) to yellowish brown (10YR 5/6) silty clay loam; very firm; massive breaking to moderately developed coarse blocky structure; indistinct boundary,	Pal 3
5.63 - 5.98	Loess: yellowish brown (10YR 5/4) silty clay loam; moderately firm; massive structure; few small soft black Fe/Mn concretions; indistinct boundary,	Loess 3
5.98 - 6.33	Palaeosol (in loess but includes some andesitic tephra deposits): yellowish brown (10YR 4/4) silty clay loam; moderately firm; massive structure breaking to moderately developed medium nutty structure; few small black Fe/Mn concretions; indistinct boundary,	Pal 4
6.33 - 6.63	Loess: yellowish brown (10YR 5/4) silty clay loam; moderately firm; massive breaking to weakly developed blocky structure; few weakly weathered ignimbrite fragments; indistinct boundary,	Pal?
6.63+ *on*	Pale grey (10YR 7/2) soft Mamaku Ignimbrite (c. ~~140 ka~~).	

* Loess and paleosol units from Eden et al. (in prep)

Note redated to 225 ka after this guide printed

The macroscopic rhyolitic tephra layers, derived from mainly the Okataina and also the Taupo volcanic centres and dated by the radiocarbon method, and the Mamaku Ignimbrite* at the base, provide the main chronology for the section via tephrochronology (Froggatt & Lowe 1990). They range from c. 140 ka* to 1.85 ka in age. Intermixed tephras in addition to those shown in Fig. 2.4, including small additions from andesitic sources, have been identified in parts of the sequence, especially in the periods from c. 130-70 ka and c. 50-20 ka (Lowe 1986; Kennedy in press). The age of the Rotoehu Ash is estimated at c. 50 ka by Froggatt & Lowe (1990); Berryman (1992) determined an age of 52 ± 7 ka based on correlation with marine terrace chronology. Others have suggested ages ranging from c. 45 ka to 64 ka (Buhay et al. 1992; Wilson et al. 1992; Kimber et al. in press). Our current preference is for an age c. 50-60 ka.

The tephric loess layers, dominantly yellowish brown (10YR 5/4-5/6), contrast with the interbedded tephras in that they have finer textures (silt to clay) and no pumice lapilli (Kennedy in press); they also have better sorting (Lowe 1981; Benny et al. 1988). They are evidently derived largely from aeolian reworked rhyolitic tephra materials. Such deposits are widespread on the Mamaku Plateau, having been first recognised by Vucetich & Pullar (1969) (see Fig. 2.6 below). The loess is dominated by subangular volcanic glass but may also contain charcoal and freshwater diatoms, consistent with accumulation during devegetated, drier and windier periods (Barratt 1988a; Kennedy 1988). An exception is the oldest loess-like layer (6.3-6.6 m; Table 2.3), which appears to have formed partly from weathering of the underlying ignimbrite (hence is referred to as a paleosol by Eden et al. in prep.). Textures range from clay in the oldest loesses (pre-140 ka) to clay loams in the younger loesses (c. 140-50 ka, units 2-3) to silt loams and fine sandy loams in the youngest loess (c. 25-15 ka, units 1a-1c). The loess layers have been matched with cold climate intervals in the marine $\partial^{18}O$ record and correlated with quartzo-feldspathic loess sequences in southern North Island (Fig. 2.4; Kennedy 1988, in press). The paleomagnetic properties of the loess were examined by Froggatt (1988), who found peaks in magnetic susceptibility corresponding to paleosols (at $\partial^{18}O$ stages 3, 5a, and 5e). Lower values related to periods of loess deposition, but Froggatt (1988) suggested that some loess (e.g. Loess 3) evidently accumulated during $\partial^{18}O$ stage 5 (the Last Interglacial).

The paleosols, developed on both tephra and loess, reflect periods of non-deposition or slow accretion when soil weathering is active. They are distinguished mainly by their darker colours, more clay, and more strongly developed structures than immediately underlying tephra or loess beds (Kennedy in press). Gradual additions of andesitic tephra appear to have enhanced soil development. The paleosols also show microstructural evidence for greater soil biotic activity under vegetation (Barratt 1988a, b). Organic and weathering processes appear to have reached a maximum in the paleosol (Paleosol 3) corresponding to late $\partial^{18}O$ stage 5 (c. 80-100 ka), where iron-rich pseudomorphs of plant fragments and abundant fine excrements suggest a forest vegetation. This phase was followed by clay mobilisation and redeposition, possibly when conditions became cooler and at least seasonally drier (Barratt 1988a). Weathering and organic activity appear to have been minimal in the loess layer corresponding to the coldest part of $\partial^{18}O$ stage 2 (c. 18-22 ka) when dust accreted rapidly. Micromorphology shows silty concentrations indicating mainly mechanical segregation and turbulence, and some associated gleying, indicating temporary water saturation, both possibly caused by seasonal freezing and thawing. Translocated clay derived from weathered minerals also suggests seasonal wetting and drying (Barratt 1988a).

A core taken adjacent to the section has recently been analysed by Kimber et al. (in press) for amino acid racemisation age determinations. D/L values (the ratio of D-amino acids to L-amino acids) for aspartic acid extracted from organic matter (by HCl and by HF on HCl residues) increased rapidly with depth and age. The HF-treated D/L values probably provide the best means of estimating the mean residence time of organic matter, and calibration against the tephrochronological ages provided a numerical age framework (Fig. 2.5; Kimber et al. in press). The ages determined largely agree with the previous estimates (Table 2.4), and provisionally fill the gaps between the Rotoehu Ash and the Mamaku Ignimbrite.

---

* The Mamaku Ignimbrite is dated at 0.14 ± 0.08 Ma (zircon fission track age) by Murphy & Seward (1981), and this age is used here. However, a new age of 0.22 Ma has recently been reported by Houghton et al. (1994).

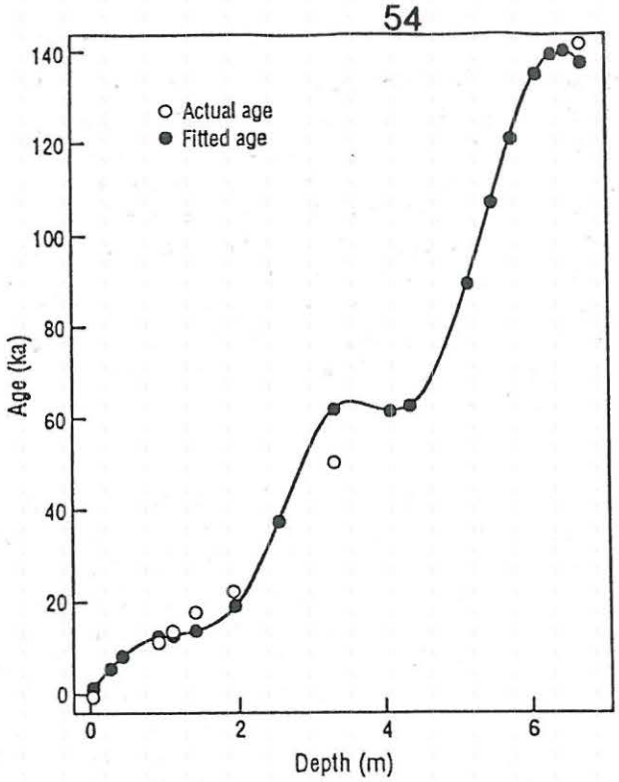

Figure 2.5: Smoothed spline describing the 'best curve' relationship between depth and age based on calibration age and corresponding D/L values at Tapapa (from Kimber et al. in press).

TABLE 2.4. Analysis of racemization data and comparison of age estimates with those from previous work (after Kimber et al. in press).

Sample No.	Deposit/palaeosol	Depth (cm)	I		Age (ka)		Previous age (ka) estimates
			Observed	Smoothed	Observed	Fitted	
0		0	0.1	0.16		1	0
2	Holocene tephra	15 – 31	0.25	0.23		5	
3	Holocene tephra	31 – 58	0.35	0.28		8	
5	Waiohau Tephra	87 – 99	0.35	0.35	11.85	12	11.85
6	Rotorua Tephra	100 – 115	0.36	0.36	13.4	13	13.4
7	Loess 1a	127 – 137	0.41	0.38		14	
9	Okareka Ash	159 – 162	–	–	18		18
12	Loess 1b	185 – 203	0.34	0.46		19	19 – 20
14	Kawakwa Tephra	203 – 248	–	–	22.5		22.5
16	Loess 1c	248 – 261	0.73	0.77		37	22.5 – 24
21	Rotoehu Ash palaeosol 2a	328 – 342	1.42	1.19		61	28 – 45
23	Rotoehu Ash	342 – 397	–	–	50		50
26	Weak Palaeosol 2b	397 – 422	1.15	1.19		61	55 – 60
27	Loess 2	422 – 450	1.07	1.2		62	65 – 75
31	Strong Palaeosol 3	508 – 536	1.59	1.65		88	80 – 110
33	Strong Palaeosol 3	542 – 567	2.07	1.95		105	80 – 110
34	Loess 3	567 – 687	1.99	2.16		117	110
37	Palaeosol 4	610 – 628	2.59	2.43		133	120 – 130
39	Loess	632 – 649	2.34	2.5		137	130 – 137
40	Loess/Pal	649 – 662	3.06	2.52		138	–
41	Ignimbrite	662 – 699	2.09	2.47	140	136	140 Recalculated to 225 ka

The full Tapapa sequence has been analysed by Eden et al. (in prep); Lowe (1986) worked on the post-Rotoehu Ash materials. Eden et al. (in prep) assayed water content, bulk density, particle size distribution, C content, sand, silt, and clay mineralogy, and major and trace elements of whole samples. In summary, the tephra layers are distinguished from one another by stratigraphic position, sand mineralogy, and major and trace element chemistry patterns. The sand mineral assemblages are dominated by glass with lesser amounts of plagioclase and cristobalite, tridymite, quartz, and kaolin subgroup aggregated clays in the felsic fractions (>91% of sand fraction); amphiboles (both calcic hornblende and cummingtonite, the latter characterising the Rotoehu Ash), clinopyroxenes, orthopyroxenes, biotite, and Fe-Ti oxides occur in varying proportions in the mafic fractions (<9% of sand fraction). Paleosols are distinguished from loess layers in being finer textured and having the lowest bulk densities, highest water contents, and highest C contents; major and trace element compositions also differ.

The <2 μm clay fractions, analysed using a combination of XRD, DTA, and acid oxalate extraction (Whitton & Churchman 1987), are dominated by kaolin subgroup minerals, likely to be mostly halloysite, and allophane (Table 2.5). In the modern soil profile, allophane ± imogolite predominate (35-63%) with kaolin minerals (3-40%) and vermiculite (10-15%, derived from biotite in the parent tephras as the vermiculite is trioctahedral; Lowe 1981), also being common. Feldspar, cristobalite, and rare quartz are also present in trace amounts. Below ≈1 m depth, kaolins increase to ≥70% and predominate throughout the rest of the section below ≈1 m, peaking in the Kawakawa and Rotoehu tephra layers (≥95%). Allophane concomitantly diminishes to only a few percent below ≈1 m depth, increasing to around 10% in Paleosol 3, Loess 3, and Paleosol 4 units between ≈4.7 m and 6.5 m (Table 2.5). Small amounts of gibbsite (≤5%) occur in beds below the Rotoehu Ash but attain about 10% in Mamaku Ignimbrite at the base of the section. The predominance of allophane in the modern soil, formed in tephra materials deposited since climatic amelioration about 14 ka, supports the notion of leaching of Si in soil solution from the upper horizons during warm, wet interglacial periods (i.e. $\partial^{18}O$ stage 1). The increase of kaolins with increase in depth suggests an increase of Si from leaching of the overlying beds. The high ratio of rhyolitic to andesitic materials at this site may have enhanced this effect (Lowe 1986). The predominance of kaolins in the section, especially during the known cold and drier periods around the time of deposition of the Kawakawa Tephra (i.e. $\partial^{18}O$ stage 2) and Loess 2 ($\partial^{18}O$ stage 4), supports the model of weak leaching of Si during glacials or stadial periods. In contrast, the increase in allophane in Paleosol 3, Loess 3, and Paleosol 4, corresponds to warmer, wetter conditions (hence promoting Si leaching) associated with the Last Interglacial between c. 90-130 ka ($\partial^{18}O$ stage 5), and matches the micromorphological evidence of Barratt (1988a) described above. Similarly, gibbsite quantities, although always small, are greatest in units of this same period (Paleosol 3, Loess 3) (Lowe & Percival 1993).

TABLE 2.5. Mineralogy (%) of clay fractions of Tapapa materials (after Eden et al. in prep).

Depth (m)	Unit*	Vermic.	Kaolin s'group†	Allophane ± imog.	Feldspar (plag.)	Cristob.	Gibbsite
0-0.15	Ap	15	25	46	7	3	
0.15-0.31	AB	15	15	47	7	3	
0.31-0.55	Bw1	15	2	63	5	2	
0.55-0.80	Bw2	15	12	51	3	1	
0.80-0.84	BC	10	40	35	3	1	
0.95-1.27	Loess 1a		80	7	3	2	<1
1.27-1.59	Rr		70-90	4-5	3	3	<1
1.59-2.03	Loess 1b		85-90	4-5	0-3	1-3	0-<1
2.03-2.48	Kk		94-97	1	0-2	2-3	
2.48-2.61	Loess 1c		90	1	2	4	
2.61-3.42	Pal 2a		85-90	5	0-2	1-4	
3.42-3.97	Re		95	1-3	0-3	0-1	
3.97-4.22	Pal 2b		90	3	3	4	<1
4.22-4.75	Loess 2		85	3-8	2-3	4-5	1-3
4.75-5.67	Pal 3		55-85	6-10	0-2	2	<1-4
5.67-6.10	Loess 3		50-70	8-10	0-2	2-3	1-5
6.10-6.49	Pal 4		55-60	10-12		4	<1-1
6.49-7.05	Mam. Ig		35-50	1-5	6-12	2-4	3-15

* Units and nos. of samples analysed: Loess 1a, 1; Rr, Rotorua Tephra, 2; Loess 1b, 4; Kk, Kawakawa Tephra, 3; Loess 1c, 1; Pal 2a, 5; Re, Rotoehu Ash, 4; Pal 2b, 1; Loess 2, 3; Pal 3, 4; Loess 3, 3; Pal 4, 3 (loess-like); Mam. Ig, Mamaku Ignimbrite, 3.
† Halloysite ± kaolinite

TABLE 2.6. Profile description and chemical data for Waiohotu gritty silt loam in the vicinity of Tapapa (from McLeod 1992).

Classification: Typic Orthic Allophanic Soil (NZSC; Hewitt 1992) (Typic Hapludand)

Profile description:

Ap1 0–12 cm
Black (10YR 2/1) gritty silt loam; non-sticky; non-plastic moderately weak in situ; few fine pores; moderately developed fine nut structure; many fine roots; indistinct wavy boundary.

Ap2 12–22 cm
Dark yellowish brown (10YR 3/4) gritty silt loam; non-sticky; non-plastic; moderately weak; few fine pores; moderately developed fine nut structure; many fine roots; indistinct wavy boundary.

Bw1 22–43 cm
Dark yellowish brown (10YR 4/6) gritty silt loam, non-sticky; non-plastic; moderately weak; abundant pores; weakly developed medium nut structure; few fine roots; diffuse wavy boundary.

Bw2 43–65 cm
Dark yellowish brown (10YR 4/6) gritty silt loam; non-sticky; slightly plastic; moderately weak; abundant pores; weakly developed medium and coarse nut structure; few dark brown (7.5YR 4/4) coatings down old root channels; diffuse boundary.

Bw3 65–90 cm
Yellowish brown (10YR 5/6) gritty silt loam; non-sticky; non-plastic; moderately weak; many pores; massive; few fine roots; indistinct wavy boundary.

2C 90–108 cm
Yellowish brown (10YR 5/8) gritty silt loam; non-sticky; slightly plastic moderately weak (but firmer than above); few coarse pores; few dark brown (7.5YR 3/4) coatings associated with old root channels; no roots; indistinct boundary.

Soil Name: WAIOHOTU GRITTY SILT LOAM — Lab No: SB10119

Horizon	Horizon depth (cm)	Lab letter	Sample depth (cm)	pH H_2O	C (%)	N (%)	C/N	Phosphorus fractions (mg %) 0.5 M H_2SO_4	Inorg.	Organic	Total	P retn (%)
Ap1	0–12	A	0–12	4.5	10.8	0.78	14	21	28	85	113	91
Ap2	12–22	B	12–22	5.4	5.7	0.37	15	14	13	45	58	98
Bw1	22–43	C	22–43	5.6	3.4	0.24	14	17	18	25	43	99
Bw2	43–65	D	43–65	5.8	1.7	0.09	19	13	16	12	28	100
Bw3	65–90	E	65–90	5.9	1.0	0.06	17	10	11	8	19	100
2C1	90–108	F	90–108	5.9	0.88	0.05	18	7	10	7	17	99
2C2	108–120+	G	108–120	5.7	1.5	0.06	25	4	8	11	19	98
Profile sample		Y	0–7.5	4.6	14.4	1.06	14	32	32	104	136	87
Composite cores		Z	0–7.5	4.5	12.3	0.89	14	24	27	90	117	89

Horizon	Horizon depth (cm)	Lab letter	Sample depth (cm)	Cation exchange (NH_4OAc @ pH7 me.%) CEC	Sum bases	%BS	Ca	Mg	K	Na	KCl ext. Al (me.%)	Exchange acidity (me.%)	Reserve Mgr (me.%)	Reserve Kc (me.%)	Phosphate ext. SO_4 (µg/g)
Ap1	0–12	A	0–12	28.2	3.57	13	2.33	0.53	0.42	0.29	1.7	59.2	0.7	0.08	1
Ap2	12–22	B	12–22	15.2	0.68	4	0.31	0.10	0.10	0.17	0.5	40.4			12
Bw1	22–43	C	22–43	9.8	0.37	4	0.16	0.04	0.06	0.11	0.1	36.9	0.6	0.06	151
Bw2	43–65	D	43–65	7.8	0.63	8	0.47	0.10	0.03	0.03	0.1	28.5			461
Bw3	65–90	E	65–90	7.1	1.30	18	0.84	0.35	0.04	0.07	0.1	25.3			568
2C1	90–108	F	90–108	6.1	0.61	10	0.30	0.24	0.03	0.04	0.0	25.4			483
2C2	108–120+	G	108–120	10.2	0.39	4	0.21	0.08	0.05	0.05	0.1	29.9			314
Profile sample		Y	0–7.5	35.2	8.61	24	6.03	1.29	0.72	0.57	1.5	82.9			2
Composite cores		Z	0–7.5	32.1	6.47	20	4.19	1.00	0.84	0.44	1.8	60.2			1

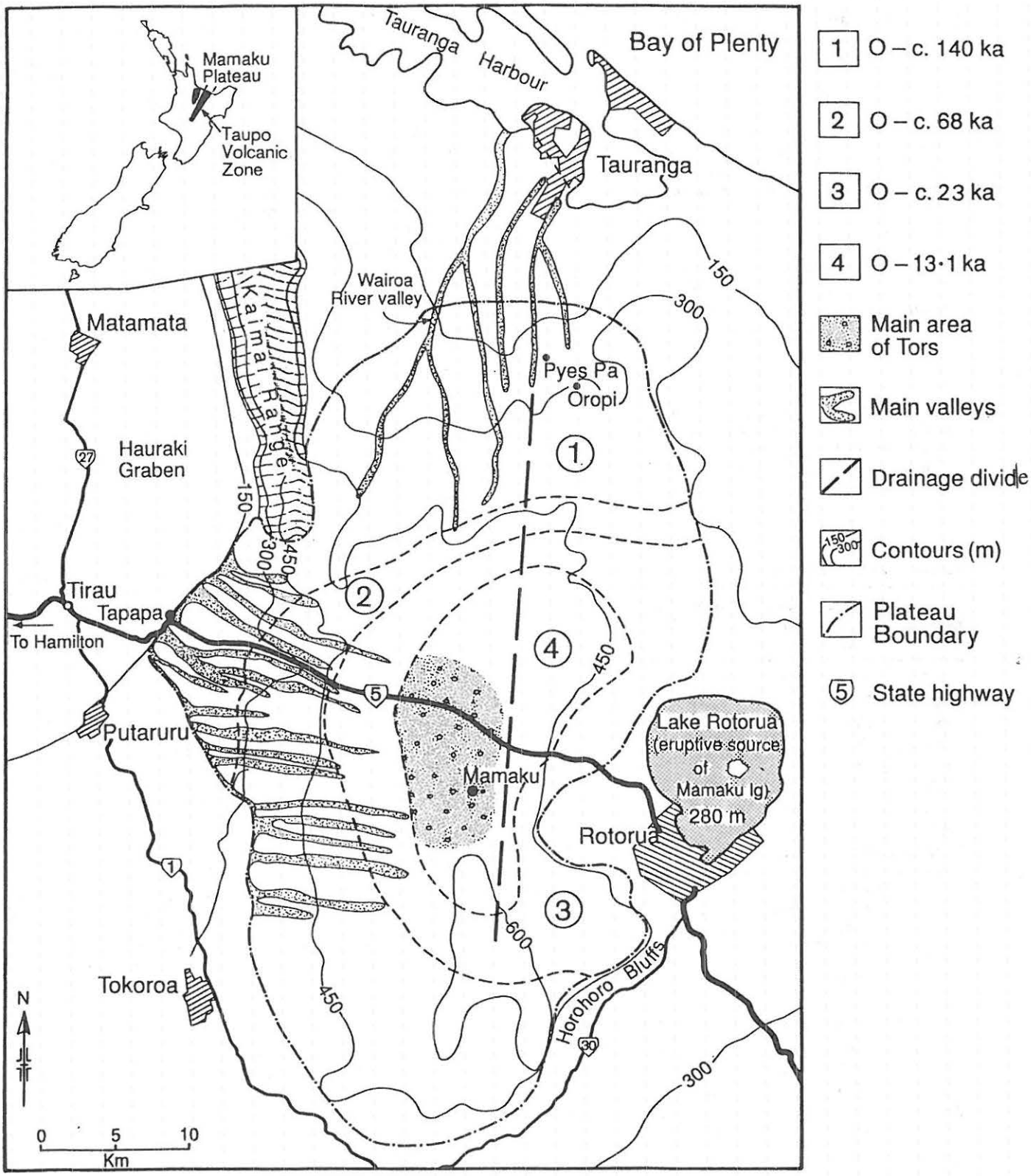

Figure 2.6: Distribution of cover bed sequences and the main geomorphic features on the Mamaku Plateau, c. 140 ka to present. Four main cover bed sequences are identified (nos. 1-4); the maximum age for each sequence is that of the marker bed immediately overlying Mamaku Ignimbrite (areas 1, 2, and 4), or that of oxygen isotope stage 4 (area 3) (from Kennedy ~~et al. in press~~).

GEOMORPHOLOGY OF MAMAKU PLATEAU AND ROTORUA BASIN

Mamaku Plateau

The Mamaku Plateau (Fig. 2.6), ≈1250 km^2 in area, lies between 150 and 650 m elevation to the west of Rotorua, but much is at ≈500 m. It has a shallow domed form, sloping gently to its margins to the west and north, but more abruptly to the east and south east. It is composed largely of densely to partly or non welded, greyish to pinkish, Mamaku Ignimbrite, often with prominent columnar jointing. The ignimbrite covers an area of >3000 km^2 and has a volume >300 km^3 (Wilson et al. 1984). The ignimbrite is up to 180 m thick near the highest part of the Plateau, thinning to <10 m towards the southern and western margins (Kennedy 1988, in press). It often directly overlies Pokai Ignimbrite (B.F. Houghton in Kennedy in press). On the crest of the Plateau (≈500-600 m), the hard ignimbrite is mostly weakly to moderately welded, the softer, less-welded ignimbrite having been eroded away (Kennedy in press). The topography is generally flat to rolling with some deeply dissected valleys and gullies, particulary to the west and north (Fig. 2.6).

The Mamaku Ignimbrite is overlain by a covering of interbedded tephras, loess, and paleosols (as at Stop 3), occasionally with dune sand as well, and these deposits have enabled detailed reconstruction of geomorphic events on the Plateau (Kennedy in press). Major erosion occurred soon after emplacement of the ignimbrite and during two intervals of cold climate: c. 68-56 ka and c. 23-15 ka (oxygen isotope stages 4 and 2, respectively; Fig. 2.4). Cover beds, especially in the southern and central part of the Plateau, were stripped and the underlying ignimbrite exposed. Widespread erosion was triggered at the beginning of these cold intervals by the destruction of the vegetative cover. Stripping of the cover beds was more severe during isotope stage 4 than stage 2, suggesting either a more extreme climate or a more fagile vegetation community during stage 4 than during stage 2, or both (Kennedy in press). The erosion produced deep valleys with cuspoid features on south-facing slopes, the cuspoid features being attributed mainly to the differential effects of cold subpolar air masses which apparently destroyed the vegetation cover on south facing slopes, triggering mass wasting or catastrophic slope failure (Kennedy in press). The main soils on the Plateau are Andic Haplohumods (Mamaku series) under rainfalls of >≈2000 mm per annum (Rijske 1979; Parfitt et al. 1981).

Near the crest of the Plateau, unusual conical hillocks or tor-like features (also referred to as inselbergs; J.D. McCraw pers. comm.) occur above ≈450 m elevation. Up to ≈10 m high, they are formed in Mamaku Ignimbrite. Such features, usually associated with old (peneplain) land surfaces, appear quite bizarre in a youthful, flat-lying volcanic landscape, and are unknown in any other ignimbrite landscapes (Kennedy in press). The tops of the tors are generally concordant. They probably represent scattered remnants of jointed ignimbrite, apparently hardened (silicified) in zones by degassing during cooling (Healy 1992). Gas pipes occur in the upper 1.5 m of soft unwelded ignimbrite forming hardened zones (Kennedy in press). The present height of the tors indicates that the Plateau crest has been reduced in elevation by at least 10 m over an area of ≈100 km^2, amounting to a volume of rock weathered and dispersed estimated at ≈1 km^3. The tors are mantled by a distinctive yellowish-orange lapilli — the Rotorua Tepha, aged c. 13 ka — and younger tephras. The surface of the underlying rock is practically unweathered, forming a smooth hard rock (in places the upper 15 cm is laminated as if shattered by frost, and a thin layer of sand sometimes occurs at the interface; J.D. McCraw pers. comm.). Freeze-thaw, wind, and fluvial processes were likely to have occurred across the ignimbrite plateau surfaces during stage 2 and possibly stage 4, although tors are absent from the latter surface (Fig. 2.6). Tor formation thus occurred during stage 2, ceasing by c. 13 ka, but may have commenced during stage 4 (Kennedy in press).

Rotorua Basin

As we descend into the Rotorua Caldera, we pass the rhyolite domes of Mt Ngongotaha (757 m), around the base of which are remnants of +90 m lake level terraces and associated diatomite that relate to the early history of Lake Rotorua, as discussed below .

Lake Rotorua was evidently formed c. 140 ka following the eruption of the Mamaku Ignimbrite and associated caldera collapse (see Fig. 2.8). The lake has an area of 80 km^2 and a maximum depth of 45 m (Lowe & Green 1992). The highest level, about 90 m above present lake level (280 m), occurred when deposits of the Rotoiti Tephra, erupted from the Okataina volcano c. 50-60 ka, blocked the northward drainage from the lake. This level is marked by extensive terraces around the lake on which part of Rotorua City is built. Tephrochonological studies show that the lake remained high until drastically lowered to near its present level c. 22 ka when the Rotoiti deposits were breached (Fig. 2.7; Kennedy et al. 1978). The lake dropped to below its present level between c. 19 and 9 ka, creating further small terraces in the process. Subsequent changes in depth, including a rise of about +10 m at c. 7 ka after the Mamaku eruption, were caused mainly by growth of the volcanic pile in the adjacent Okataina Volcanic Centre (Nairn 1989). Since then, lake levels have steadily dropped, probably because of downcutting at the Ohau outlet. The higher lake levels between c. 7 and 4 ka may have partly resulted from higher rainfall than at present (McGlone 1983). Mokoia Island in Lake Rotorua is a rhyolite dome.

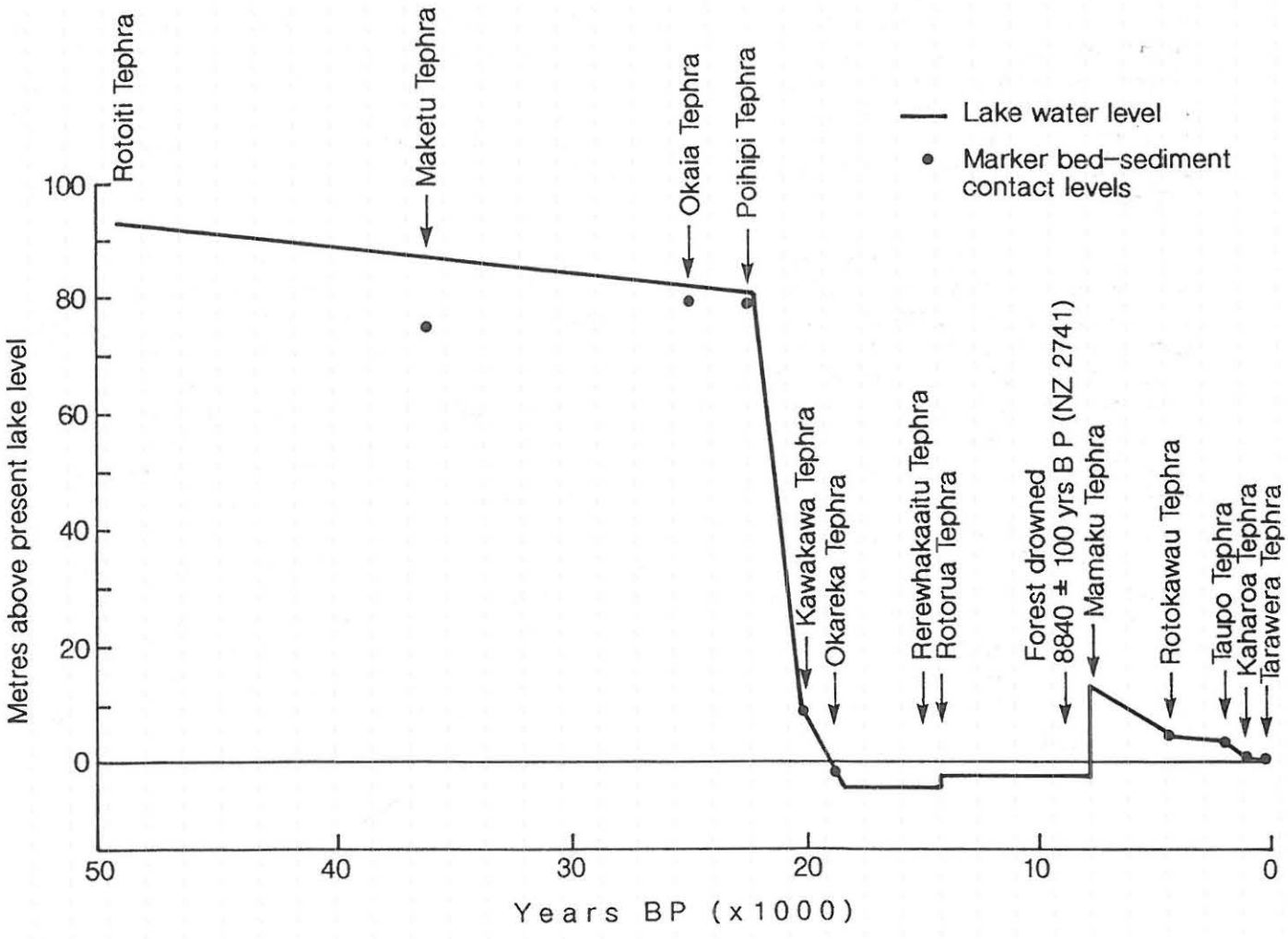

Figure 2.7: Variations in water levels of Lake Rotorua from c. 50-60 ka to the present based on tephrochronology. Present lake level is 280 m a.s.l. From Lowe & Green (1992) based on Kennedy et al. (1978) and Nairn & Wood (1987).

OKATAINA VOLCANIC CENTRE AND LATE QUATERNARY TEPHRAS

The Okataina volcano is the most recently active of the TVZ rhyolitic centres and, with Taupo volcano, one of the two most productive rhyolite volcanoes known (Nairn 1989; Wilson 1993). Lying to the east of Rotorua Caldera (Fig. 2.8), it has been active from c. 380 ka, but since the eruption of the Rotoiti Tephra c. 50 ka, the Haroharo and Tarawera volcanic complexes have grown on the caldera floor, formed by the overlapping of multiple collapse structures associated with a succession of voluminous (>100 km3) pyroclastic eruptions. A clear age distinction exists between the exposed eruptives within the caldera, all <22 ka, and the rocks forming the caldera margins, all >140 ka (Nairn 1989). Nairn (1989) and Nairn & Wood (1987) describe the early deposits in detail.

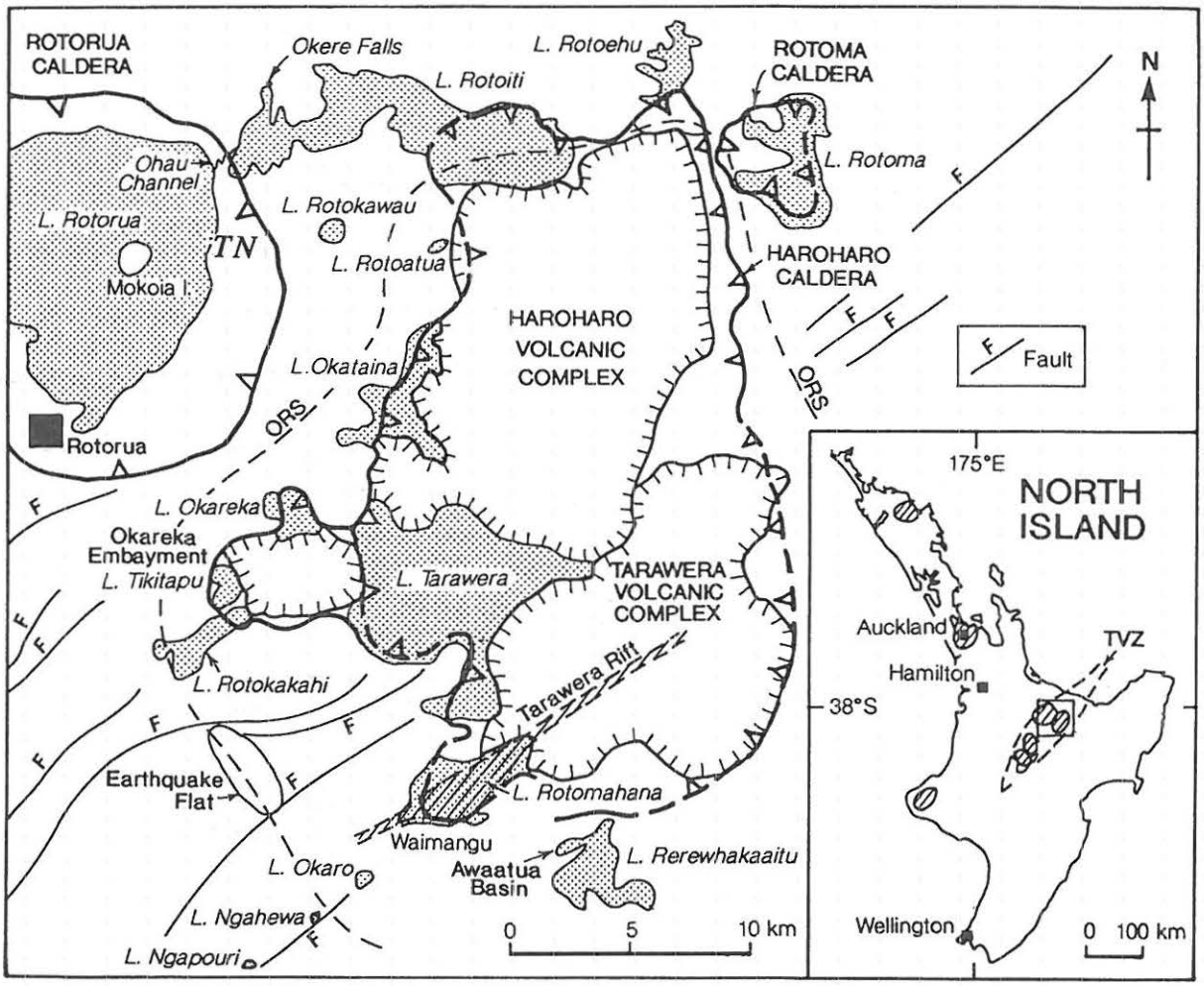

Figure 2.8: Structural and volcanic features of the Rotorua area associated with the Rotorua and Haroharo calderas. The latter lies within the Okataina Volcanic Centre (marked by ORS, the Okataina Ring Structure). After Nairn (1989). TN = Te Ngae site (Stop 5).

There have been 11 eruptive episodes during the past c. 22 ka from vents in the Haroharo and Tarawera complexes, separated by quiescent periods lasting up to a few thousand years (Table 2.7; Nairn 1989, 1992). All were rhyolitic except for several basaltic events, including the most recent (and one of the smallest), the Tarawera-Rotomahana-Waimangu eruption on 10 June 1886 (Walker et al. 1984). The erupted volumes of pyroclastic material are relatively uniform, varying from ≈1 to 15 km^3. A generalised map of the lavas and major pyroclastic deposits of the Haroharo Volcanic Complex is given in Fig. 2.9; the stratigraphy and chronology of these are summarised in Table 2.8.

TABLE 2.7. Sequence of intracaldera eruptions at Okataina (post-22 ka) with estimated volumes. All are rhyolitic apart from the named basalts, although the Okareka and Kaharoa eruptives also contain a basalt component (from Nairn 1989).

Eruptive episode	age (yrs B.P.)	Lava volume (km^3)	Pyroclastics volume (km^3)	Equivalent magma volume (km^3) Haroharo	Tarawera
Tarawera Basalt (1886 A.D.)			2[1]	--	0.7
Kaharoa	c. 800	2.5	5	--	5
Rotokawau Basalt[2]	c. 3500		0.7	0.5	--
Whakatane	c. 5500	9	10	13	--
Mamaku	c. 7500	15	6	17.5	--
Rotoma	c. 9000	2	13	8	--
Waiohau	c. 11000	4	14.5	--	10.5
Rotorua	c. 13500	1	7	4	--
Rerewhakaaitu	c. 15000	2	6	--	5
Okareka	c. 18000?	5	5	--	7
Te Rere	c. 21000	7.5	3	9	--
			Totals	52	28.2
				c. 80	

Notes
1 Walker et al. 1984.
2 Strictly not an intracaldera eruptive.

TABLE 2.8. Stratigraphy and chronology of Haroharo Volcanic Complex lavas and pyroclastics shown on Fig. 2. 9. From Nairn (1989).

Eruptive episode and age (yrs B.P.)	Lavas	Pyroclastics
Whakatane	Tikorangi dome	
c. 5500	Makatiti dome	Minor pyroclastic eruptions
	Haroharo dome	
	Makatiti lava flows	
	Rotokohu dome	
	Okataina lava flow	Rotokohu tuff cone
	Tapahoro dome	Whakatane Ash (plinian)
	Tapahoro lava flows	Whakatane Pyroclastics
	Rotoroniu lava flows	
Mamaku		Te Whekau explosion breccia
c. 7500	Te Horoa dome	Local flow and surge deposits
	Hainini dome	
	Hainini lava flow	
	Te Matae lava flow	
	Parewhaiti dome	
	Ruakokopu lava flow	Hainini Pyroclastics
	?Otangimoana lava flow	
	?Oruaroa lava flow	Mamaku Ash (plinian)
	Waiti lava flow	
	Kaipara lava flow	
Rotoma	Te Pohue lava flows	?Otamuri Pyroclastics
c. 9000		Tuahu Pyroclastics
	Rotoma lava flow[1]	Rotoma Ash (plinian)[1]
Te Rere	Haumingi lava flow	
c. 21000	Te Koutu lava flow	?Tapuaeharuru Pyroclastics
	Tuarae lava flow	?Te Haehaenga Pyroclastics
	?Fenton's Mill lava flow	Te Rere Ash (plinian)

Notes
1 From Rotoma Caldera

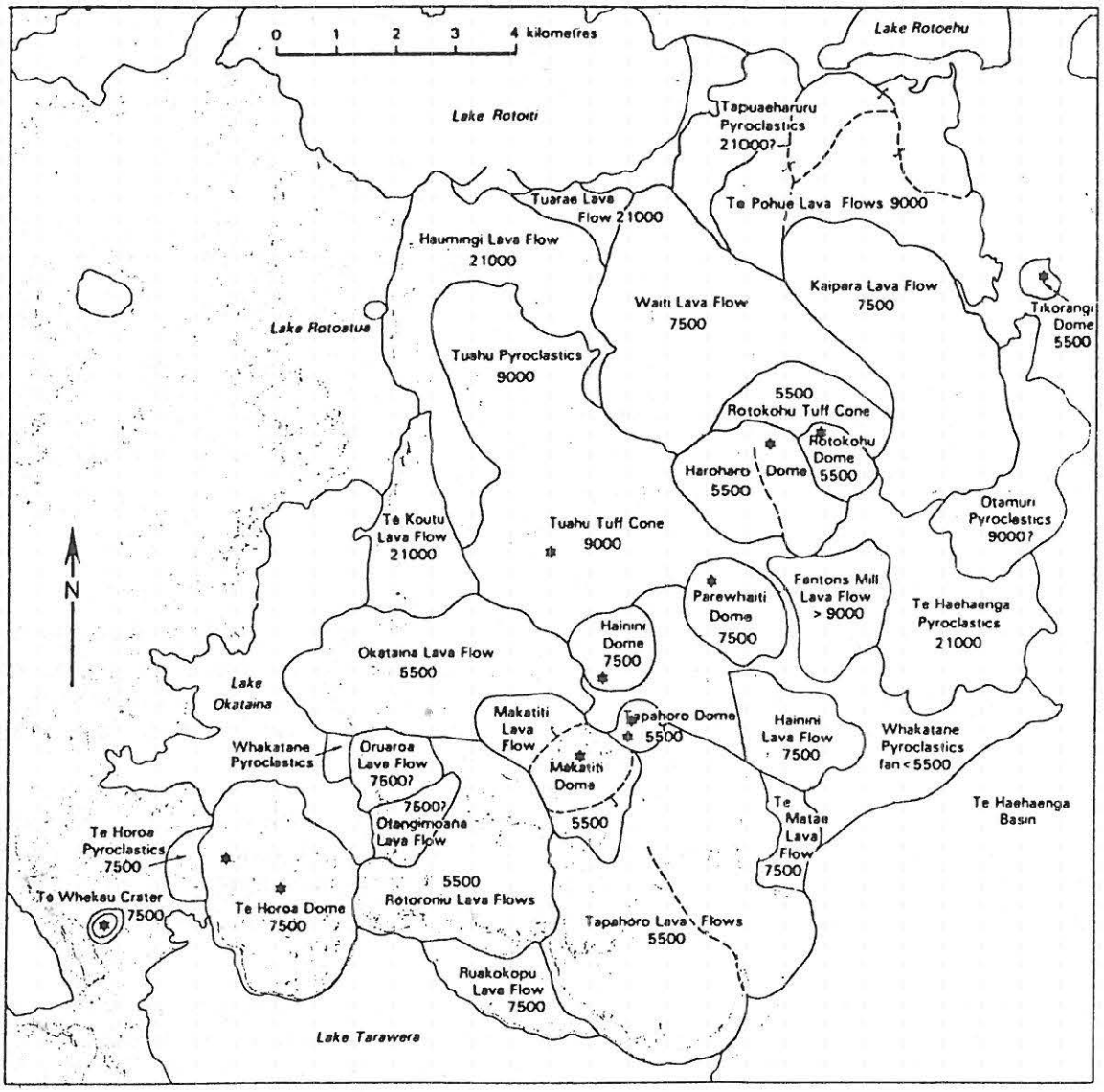

Figure 2.9: Generalised map of Haroharo Volcanic Complex lavas and major pyroclastic deposits. See Table 2.8 for correlation with eruption episodes (from Nairn 1989).

STOP 5 — Te Ngae Section (U15/018418) [Please be especially careful of traffic]

The Te Ngae section occurs alongside Highway 33 near Te Ngae on a sub-vertical terrace cliff face a few hundred metres east of Lake Rotorua. The 6-m high exposure lies at 300 m altitude, and the site has a mean annual rainfall of 1490 mm with a mean annual temperature of 11.9°C. Native vegetation from c. 9 ka to 1 ka was a *Dacrydium cupressinum* (rimu)-dominant podocarp-hardwood forest, with Polynesian fires since c. 1 ka reducing the forest cover to fernland, grass and scrub by 400 years ago (McGlone 1983). The modern soil is formed from multiple tephra layers including Rotomahana Mud, Kaharoa Tephra, Taupo Tephra, and Rotokawau Tephra overlying earlier eruptives (Fig. 2.10). It is mapped as the Rotoiti series (Rijske 1979), an ashy, mesic, Humic Udivitrand.

The section comprises 11 major tephra deposits aged from 1886 A.D. to c. 18 ka, most being derived from either the Haroharo or Tarawera complexes within the Okataina Volcanic Centre (Figs. 2.8, 2.10). 'Dustings' of tephras from other centres are likely to be present but are minor (Birrell & Pullar 1973; Green 1987). The basal tephra exposed is the Okareka Tephra (aged c. 18 ka), which lies interbedded with tephric loess overlying lake sediments. All the tephras have been dated by the radiocarbon method except Okareka, the age of which is well constrained stratigraphically (Froggatt & Lowe 1990; Nairn 1992). The terrace on which the tephras lie relates to higher lake levels, with the highest stand (+ ≈10 m) in recent times occurring c. 7 ka following the Mamaku eruption. This would correspond today to a position at about the foot of the exposure. A brief description of the section is given in Table 2.9. Note that several of the paleosols at the Te Ngae section (e.g. Rotoma, Taupo) are not as well preserved as at other sites in the area.

Analyses of Tephras and Paleosols

The weathering of tephras and associated paleosols at this site, and several other sites in the Rotorua region, have been studied in detail by Green (1987). Part of the study examined the kinetics of glass weathering and implications for the formation of clay minerals, as described in Hodder et al. (1990). Similarly, an associated project for determining volcanic glass content in tephra-derived soils or paleosols using HF dissolution is reported by Lowe & Green (1992a).

The tephra sand and silt fractions are dominated by glass with plagioclase, quartz, and cristobalite making up the remainder of the felsic fractions (≥≈95% of the sand fraction), with ferromagnesian minerals (hypersthene, augite, biotite, calcic hornblende, cummingtonite, apatitie, and zircon) and Fe-Ti oxides (titanomagnetite) dominating the mafic fractions (≤≈5% of the sand fraction). The glass is highly siliceous (74-77% SiO_2 on a hydrous basis; Stokes et al. 1992).

The paleosols, notably the buried Bw horizons, were analysed using a variety of methods, and Green (1987) found that these tend to have lower bulk density, higher organic C%, and generally finer textures and higher clay contents than associated parent tephra materials. Although generally only weakly weathered, the degree of development of the paleosols, as indicated by wt% allophane on a whole sample basis and in the silt fraction, wt% clay, clay:sand ratio, and, to a lesser extent, by bulk density, is significantly correlated with effective time for weathering (i.e. time between successive eruptions). Fig. 2.11 demonstrates the relationship between time for weathering and clay content of buried Bw horizons on tephras in the Rotorua area (Lowe & Percival 1993). The time for weathering is greatest for the paleosol on Waiohau Tephra (c. 3320 years) and least for that on Kaharoa Tephra (c. 670 years) (Hodder et al. 1990). Such a correlation assumes that there is minimal 'contamination' of the paleosols by andesitic components (cf. Stop 10, Post-Conference Tour Day 1).

The secondary mineral assemblages and clay fractions were analysed using oxalate and pyrophosphate extraction techniques together with IR, DTA, and XRD analysis. The allophane and ferihydrite contents on a whole soil basis are given in Table 2.10, allophane and ferrihydrite ranging up to 13.5% and 4.4%, respectively (in the basaltic Rotokawau Tephra paleosol). The whole sample analyses of allophane closely match the sum of analyses on separate fractions (Lowe & Percival 1993). These latter results emphasise the common occurrence of pedogenic aggregated clay in silt- and sand-sized fractions in tephra materials.

TABLE 2.9. Description of the Te Ngae section (after Green 1987).

A_p	0-18 cm	black(7.5YR 2/1)sandy clay, diffuse irregular boundary (Rotomahana Mud)
C	18-20	greyish yellow(2.5Y 6/2)sand, indistinct discontinuous boundary (Rotomahana Mud)
2uA	21-31	black(10YR 2/1)sandy loam, many pumice clasts, distinct irregular boundary (Kaharoa Ash)
2uBw	31-55	brownish black(7.5YR 3/2)loamy sand, abundant pumice, indistinct irregular boundary (Kaharoa Ash)
2uC	55-60	light grey(10YR 8/1)pumice lapilli, distinct discontinuous boundary (Kaharoa Ash)
3uBC	60-70	dark brown(7.5Y 3/4)sandy loam, soft vesicular pumice, diffuse discontinuous boundary (Taupo Pumice)
4uBw	70-80	brown(10YR 4/6)silt loam, few basalt fragments, indistinct irregular boundary (Rotokawau Ash)
4uC	80-100	grey(10YR 5/1)firm basalt, distinct irregular (Rotokawau basalt)
5uBw	100-110	brown(10YR 4/4)sandy loam, distinct irregular boundary (Whakatane Ash)
5uC	110-120	greyish yellow(2.5Y 7/2)coarse sand, indistinct wavy boundary (Whakatane Ash)
6uBw	120-135	yellowish brown(10YR 5/8)sandy loam, diffuse irregular boundary (Mamaku Ash)
6uBC	135-160	bright yellow brown(2.5Y 7/6)loamy sand, diffuse wavy boundary (Mamaku Ash)
6uC	160-183	light yellow(2.5Y 7/4)coarse sand, indistinct irregular boundary (Mamaku Ash)
6uC	183-194	dull yellowish brown(10YR 5/4)fine sand, discontinuous distinct boundary (Mamaku Ash)
6uC	194-220	light grey(2.5Y 7/1)coarse sand, distinct irregular boundary (Mamaku Ash)
6uC	220-230	light yellow(2.5Y 7/4)medium sand, distinct discontinuous boundary (Mamaku Ash)
6uC	230-234	dull yellowish orange(10YR 7/2)very fine sand, distinct discontinuous boundary (Mamaku Ash)
7uBw	234-275	dull yellow(2.5Y 6/4)loamy sand, distinct irregular boundary (Rotoma Ash)
7uBC	275-293	light yellow(2.5Y 7/3)fine loamy sand, distinct regular boundary (Rotoma Ash)
7uC	293-308	light brownish grey(7/2)medium sand, distinct irregular boundary (Rotoma Ash)
7uC	308-310	light yellow(2.5Y 7/3)fine sand, distinct irregular boundary (Rotoma Ash)
8uBw	310-330	dull yellow orange(10YR 6/4)sandy loam, diffuse wavy boundary (Waiohau Ash)
8uBC	330-346	dull yellow orange(10YR 7/3)loamy sand, diffuse wavy boundary (Waiohau Ash)
8uC	346-366	light yellow(2.5Y 7/3)coarse sand, indistinct irregular boundary (Waiohau Ash)
9uBw	366-384	dull yellow orange(10YR 6/3)sandy loam, indistinct wavy boundary (Rotorua Ash)
9uBC	384-395	dull yellow(2.5Y 6/3)fine sand, distinct wavy boundary (Rotorua Ash)
9uC	395-414	light yellow(2.5Y 7/3)showerbedded coarse sand, distinct smooth boundary (Rotorua Ash)
9uC	414-417	light yellow orange(10YR 8/4)fine sand, distinct wavy boundary (Rotorua Ash)
9uC	417-444	light yellow (2.5Y 7/4)showerbedded ash normally grading from fine sand to coarse lapilli, distinct smooth boundary (Rotorua Ash)
10uBw	444-458	dull yellow orange(10YR 6/4)sandy loam, distinct wavy boundary (Rerewhakaaitu Ash)
10uBC	458-468	greyish yellow(2.5Y 7/2)med sand, indistinct diffuse boundary (Rerewhakaaitu Ash)
10uCg	468-476	dull yellow orange(10YR 6/4)fine sand, regular distinct boundary (Rerewhakaaitu Ash)
11uC	476-512	dull yellow orange(10YR 6/3)silt loam, indistinct irregular boundary (tephric loess)
12uBC	512-524	dull yellow orange(10YR 6/4)loamy sand, diffuse wavy boundary (Okareka Ash)
13uC	524-563	dull yellow brown(10YR 5/4)silt loam, diffuse irregular boundary (tephric loess)
14uBw	563-570	dull yellowish brown(10YR 5/4)loamy sand (lake sediments)

Note: Horizon notation 'u' here indicates a buried horizon

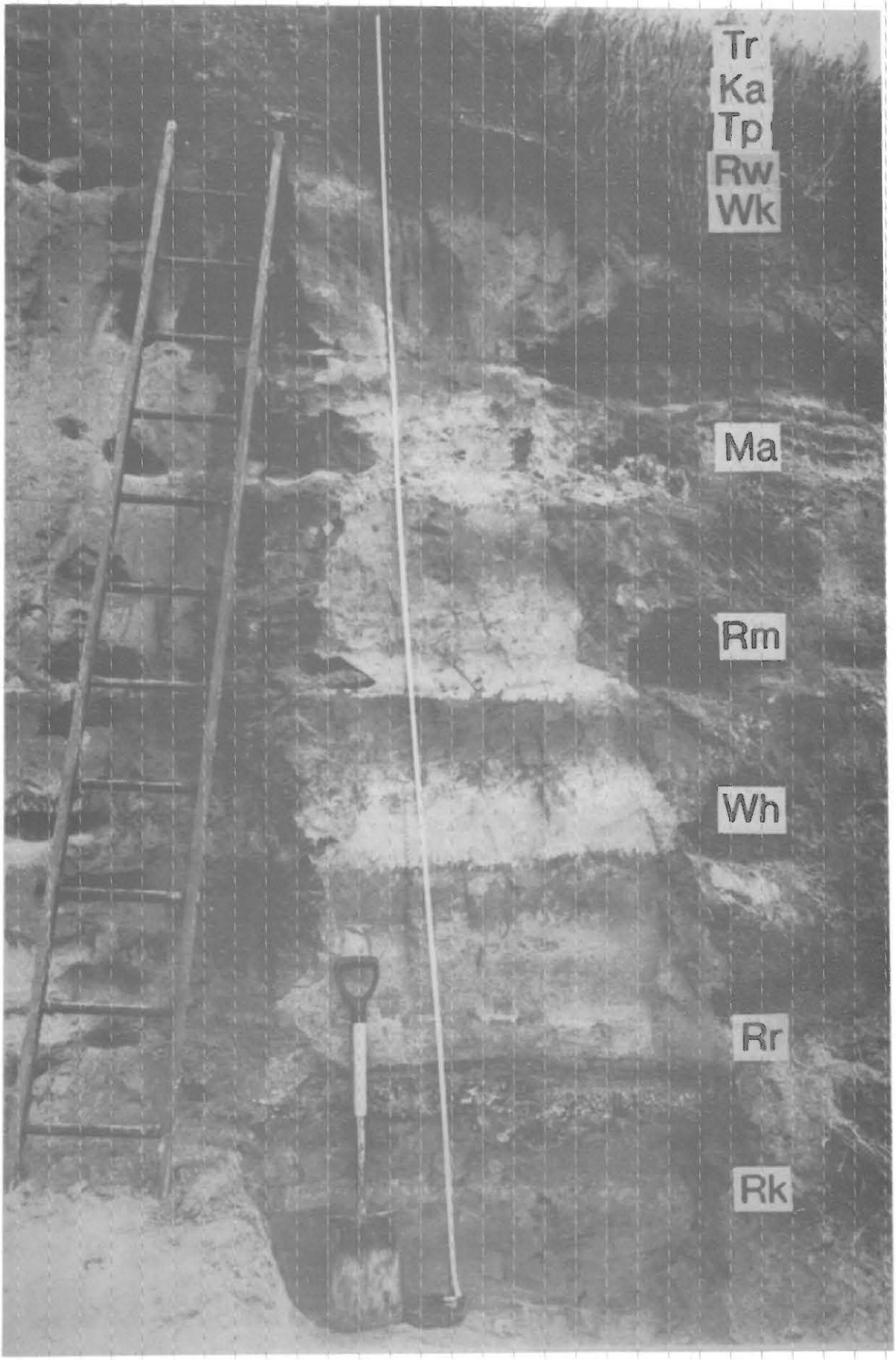

Figure 2.10: Sequence of late Quaternary tephra deposits and paleosols at Te Ngae Road section. Tephra formations and ages (from Froggatt & Lowe 1990) are: Rk, Rerewhakaaitu, 14.7 ka; Rr, Rotorua, 13.1 ka; Wh, Waiohau, 11.9 ka; Rm, Rotoma, 8.5 ka; Ma, Mamaku, 7.3 ka; Wk, Whakatane, 4.8 ka; Rw, Rotokawau, 3.5 ka (basaltic), Tp, Taupo. 1.85 ka; Ka, Kaharoa, 700 yr ago; Tr, Tarawera (Rotomahana Mud), 1886 A.D. Okareka Tephra (c. 18 ka) also occurs in the section in tephric loess below Rk. All the tephras except Tp (from Taupo volcano) are derived from Okataina volcano. Photo: B.E. Green.

TABLE 2.10. Clay content and allophane, ferrihydrite, and halloysite content of whole samples at Te Ngae (after Green 1987).

Tephra#	Hor.	Clay% (<2 μm)	Alloph.* wt%	Ferrih.* wt%	Halloy.† wt%
Tr	Ap	nd	2.0	1.3	
Ka	2A	6.1	2.7	1.3	
	2Bw	6.5	2.6	1.4	
	2Cu	0.9	0.8	neg	
Rw	4Bw	nd	13.5	4.4	
	4Cu	nd	8.9	3.7	
Wk	5Bw	7.1	6.4	1.8	
	5BC	3.8	4.5	1.1	
	5Cu	2.4	2.5	0.2	
Ma	6Bw	8.8	6.7	1.3	
	6BC	4.5	5.5	0.3	
	6Cu1	2.0	1.9	neg	
Rm	7Bw	3.7	3.3	0.2	
	7BC	4.2	5.5	0.2	
Wh	8Bw	13.6	9.2	1.0	4.7
	8BC	7.6	7.4	0.1	nd
	8Cu	3.5	5.3	neg	nd
Rr	9Bw	8.6	6.2	0.2	4.2
	9BC	5.3	5.5	0.1	nd
	9Cu1	2.1	3.7	neg	nd
Rk	10Bw	8.2	1.3	0.7	5.6
	10BC	6.1	1.6	0.5	nd
	10Cg	3.8	1.0	neg	nd
Ok	12BC	nd	1.4	0.1	nd

Abbreviations explained in Fig. 2.10.
* Allophane and ferrihydrite estimated using acid oxalate and pyrophosphate extractions of Al, Si, Fe
† Halloysite estimated using DTA; neg = neglible; nd = not determined

TABLE 2.11. Clay mineral assemblages inferred from IR spectroscopy data for clay fractions in paleosols (Bw horizons) at Te Ngae, Democrat Rd, and Tikitere sections near Rotorua (after Green 1987).

Paleosol	Te Ngae	Democrat Rd Tikitere[T]
Ka	GL ≥Al- & Si-ALL >OM >>H, Q, +	
Tp		Al-ALL >GL > OM >>H, +
Wk	Al-ALL >Si-ALL ≥GL >OM > H, +	[T]Al-ALL >Si-ALL >GL >OM, H, Q, +
Ma	Al-ALL >Si-ALL >GL >OM, FE, H, +	
Rm		Al-ALL >GL > OM >Si-ALL >H, +
Wh	H ≥Si-ALL >GL >>OM, Al-ALL, +	Al-ALL >Si-ALL ≥GL >H >Q, +
Rr	Si-ALL >Al-ALL ≥GL ≥H >>OM, +	H >GL >Si-ALL > OM, +
Rk	H >GL >Si-ALL >OM, Al-ALL, +	

GL, glass; Al- and Si-ALL, Al-rich and Si-rich allophane; H, halloysite; OM, organic matter; FE, iron oxide mineral (e.g. ferrihydrite); Q, quartz; +, other Al and Si phase minerals (e.g. quartz, cristobalite, gibbsite).

The clay fractions may contain a combination of Al-rich and Si-rich allophane, halloysite, volcanic glass, organic matter, oxides and hydroxides of Fe (including ferrihydrite), Al (gibbsite), and Si, and minor crystalline primary (residual) minerals; a summary is given in Table 2.11 (based mainly on IR data and including results of analyses from nearby Tikitere [U15/053436] and Democrat Road [V16/141150] sites). Al-rich allophane predominates in the paleosols on the Te Ngae tephras deposited after Waiohau Tephra in the sequence (i.e. since c. 12 ka). At the same time, halloysite occurs in negligible quantities in these beds, instead occurring in appreciable quantities in paleosols with significant Si-rich allophane structures on the Waiohau, Rotorua, and Rerewhakaaitu tephras. The genesis of these clays essentially accords with the inferred paleoclimatic regime operative during the effective period of weathering at the land surface — climate was windier, drier and colder than present from c. 18 ka to about 12 ka, becoming moister and warmer from c. 12 ka to 8.5 ka or later, then becoming slightly drier and frostier with minor fluctuations in temperature to c. 1850 years ago, and finally attaining present day status (e.g. McGlone 1983, 1988; Newnham et al. 1989; Pillans et al. 1993). Thus conditions for the period from c. 18 ka to about 12 ka were conducive to the formation of halloysite and Si-rich allophane (as in the Rerewhakaaitu paleosol) whereas after about 8.5 ka the conditions favoured stronger leaching and the formation of Al-rich allophane (as in the Rotoma, mamaku, Whakatane, Taupo, and Kaharoa paleosols). However, variations in clay mineral assemblages between the Te Ngae and Democrat Rd sites (Table 2.11) for the Waiohau and Rotorua paleosols suggests that localised microenvironmental variations, such as perching due to textural changes, or some post-burial modification, have affected these (Green 1987).

The micromorphology of the paleosols from Whakatane to Rerewhakaaitu tephras has been studied by Bakker et al. (1994). Sase et al. (1988) studied opal phytoliths in the section.

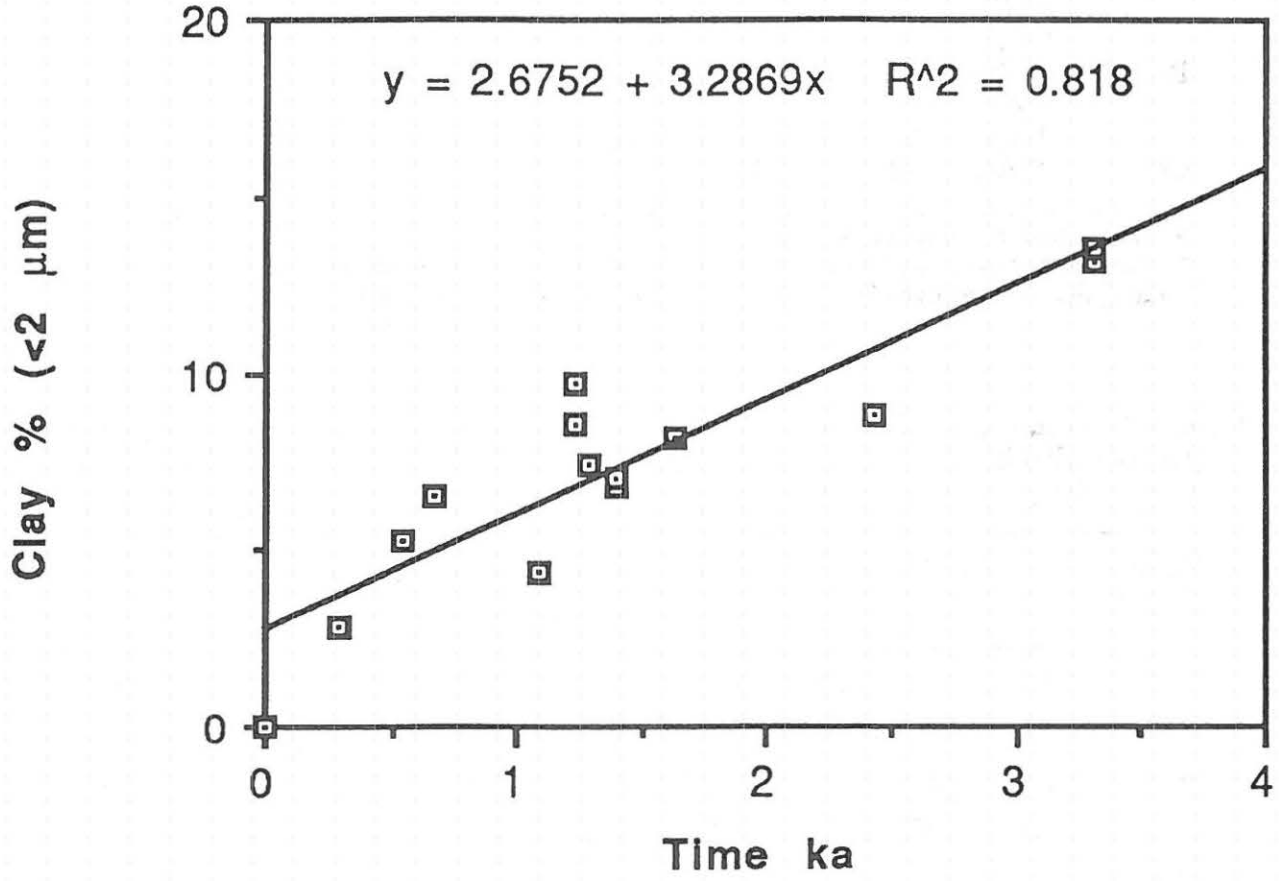

Figure 2.11: Relationship between time for weathering of buried paeosols and clay content (based on data in Green 1987)

The kinetics of clay formation can be described in terms of a combination of parabolic and linear kinetics, reflecting the hydration of glass and the formation of clay minerals, respectively (Hodder et al. 1990). Such a two-stage model is consistent with the formation of clay minerals showing an Arrhenian temperature dependence and suggests, on the basis of calculated activation energies, that the process of formation of Al-rich allophane is diffusion controlled, whereas the rate of formation of Si-rich allophane is controlled by the chemical processes at the site of reaction (Hodder et al. 1990). This model is particularly appropriate for buried paleosols from tephra deposits such as those at Te Ngae where the time for weathering is comparatively short (a few hundred to few thousand years) and contamination is minimal. The rate constant calculated for the weathering of rhyolitic tephras in the Rotorua area is 1.23 ka^{-1}, and the half-life of the glass is c. 18 ka (Green 1987).

STOPS 6,7, & 8 — Holocene Tephra Sections, Haroharo Caldera

Three exposures will be visited along Rototiti Road in the Rotoiti Forest. We have allowed about 40 minutes per stop (including travel in between). After turning off from Gisborne Point, Lake Rotiti (Fig. 2.1), we initially ascend over the toes of the oldest lavas (c. 21 ka) in the Haroharo Caldera (Fig. 2.9, Table 2.8). As the road continues to climb towards the centre of the Haroharo Caldera, the tephras mantling the lavas temd to thicken and coarsen, especially the Rotoma (c. 9 ka), Mamaku (c. 7 ka), and Whakatane (c. 5 ka) eruptives.

STOP 6 — Section A (V15/134046)

This sections shows interbedded fall and (poorly sorted) flow units of the Mamaku Pyroclastics (c. 7 ka) uncomformably overlying strongly eroded Rotoma (= Tuahu; Table 2.8) (c. 9 ka) deposits. The section is located ≈5 km north of the presumed Mamaku vent (Nairn & Wood 1987). Kaharoa deposits (0.7 ka) occur at the top of the section.

STOP 7 — Section B (V15/142044)

This long section shows pyroclastic surge beds, associated co-surge ashes(?), and interbedded fall deposits of the Rotoma-Tuahu (c. 9 ka) eruptive episode from adjacent source vent. Gullies developed in the Rotoma deposits are infilled by Mamaku (c. 7 ka) deposits. Further along the section occasional ballistic blocks, overlying Rotoma surge deposits, mark the base of the Whakatane (c. 5 ka) deposits.

STOP 8 — Section C (V16/173377)

This section is located between the Haroharo Dome (817 m), the source vent for the Whakatane eruptive episode (c. 5 ka), and the 'Ridgetop' domes (651 m). The section exposes essentially planar pyroclastic beds of the Mamaku (c. 7 ka) eruptive episode; these have been eroded and a paleosol has developed on them. Draping the Mamaku deposits are tephra beds of the Whakatane eruptive episode (c. 5 ka). Locally thick Kaharoa (c. 0.7 ka) and Tarawera (AD 1886) basaltic deposits occur at the SE end of the section; both these are derived from Tarawera volcano (1111 m) which is about 12-14 km to the S.

STOP 9 — Overview of Rotorua and Haraoharo calderas, Mt Ngongataha (U16/915381)

Aorangi Peak Restaurant is at 580 m elevation. If the weather is good, we shall have panoramic views of Rotorua City (population ≈55 000), Lake Rotorua, and the rhyolite domes of Mt Tarawera in Haroharo Caldera (Fig. 2.8).

REFERENCES

Bakker, L.; Lowe, D.J.; Jongmans, A.G. 1994: A micromorphological investigation of alteration of tephra material and neoformation of clay minerals in a chronosequence of rhyolitic tephras and buried paleosols, North Island, New Zealand. *Programme and Abstracts*, International Inter-INQUA Field Conference and Workshop on Tephrochronology, Loess, and Paleopedology, Hamilton, New Zealand (in press).

Barratt, B.C. 1988a: Micromorphology and pedogenesis in a Late Pleistocene succession of tephric loesses and paleosols near Tapapa, Mamaku Plateau, North Island, New Zealand (Abstract). *In* Eden, D.N.; Furkert, R.J. (eds) Loess: Its Distribution, Geology and Soils. A.A. Balkema, Rotterdam: 7-8.

Barratt, B.C. 1988b: Micromorphological descriptions of tephric loess and paleosol layers in the Tapapa section, Mamaku Plateau, North Island, New Zealand. *New Zealand Soil Resources report SR16.* 35p.

Benny, L.A.; Kennedy, N.M.; Kirkman, J.H.; Stewart, R.B. 1988: Mineralogical and textural discriminantion of loess derived from a tephra near Rotorua, New Zealand. *Australian journal of soil research 26*: 301-312.

Berryman, K. 1992: A stratigraphic age of Rotoehu Ash and late Pleistocene climate interpretation based on marine terrace chronology, Mahia Peninsula, North Island, New Zealand. *New Zealand journal of geology and geophysics 35*: 1-7.

Birrell, K.S.; Pullar, W.A. 1973: Weathering of paleosols in Holocene and late Pleistocene tephras in central North Island, New Zealand. *New Zealand journal of geology and geophysics 16*: 687-702.

Black, P.M.; Briggs, R.M.; Itaya, T.; Dewes, E.R.; Dunbar, H.M.; Kawasaki, K.; Kuschel, E.; Smith, I.E.M. 1992: K-Ar age data and geochemistry of the Kiwitahi Volcanics, western Hauraki Rift, North Island, New Zealand. *New Zealand journal of geology and geophysics 35*: 403-413.

Briggs, R.M. 1986: Petrology and geochemistry of Maungatautari, a medium-K andesite-dacite volcano. *New Zealand journal of geology and geophysics 29*: 273-289.

Briggs, R.M.; Gifford, M.G.; Moyle, A.R.; Taylor, S.R.; Norman, M.D.; Houghton, B.F.; Wilson, C.J.N. 1993: Geochemical zoning and eruptive mixing in ignimbrites from Mangakino volcano, Taupo Volcanic Zone, New Zealand. *Journal of volcanology and geothermal research 56*: 175-203.

Buhay, W.M.; Clifford, P.M.; Schwarcz, H.P. 1992: ESR dating of the Rotoiti Breccia in the Taupo Volcanic Zone, New Zealand. *Quaternary science reviews 11*: 267-271.

Cas, R.A.F.; Wright, J.V. 1987: Volcanic Successions. Allen & Unwin, London. 528p.

de Lange, P.J.; Lowe, D.J. 1990: History of verical displacement of Kerepehi Fault at Kopouatai bog, Hauraki Lowlands, New Zealand, since c. 10 700 years ago. *New Zealand journal of geology and geophysics 33*: 277-283.

Eden, D.N.; Hunt, J.L.; Whitton, J.S.; Kennedy, N.M.; Lowe, D.J. in prep: Element chemistry, mineralogy, and other properties of a 140 000 year old tephra, loess, and paleosol sequence from Mamaku Plateau, central North Island, New Zealand. Unpublished manuscript.

Froggatt, P.C. 1988: Paleomagnetism of Last Glacial loess from two sections in New Zealand. *In* Eden, D.N.; Furkert, R.J. (eds) Loess: Its Distribution, Geology and Soils. A.A. Balkema, Rotterdam: 59-68.

Froggatt, P.C.; Lowe, D.J. 1990: A review of late Quaternary silicic amd some other tephra formations from New Zealand: their stratigraphy, nomenclature, distribution, volume, and age. *New Zealand journal of geology and geophysics 33*: 89-109.

Froggatt, P.C.; Nelson, C.S.; Carter, L.; Griggs, G.; Black, K.P. 1986: An exceptionally large late Quaternary eruption from New Zealand. *Nature 319*: 578-582.

Green, B.E. 1987: Weathering of buried paleosols on late Quaternary rhyolitic tephras, Rotorua region, New Zealand. Unpublished MSc thesis, University of Waikato, Hamilton.

Green, J.D.; Lowe, D.J. 1985: Stratigraphy and development of c. 17 000 year old Lake Maratoto, North Island, New Zealand, with some inferences about postglacial climatic change. *New Zealand journal of geology and geophysics 28*: 675-699.

Hayward, B.W. 1987: Granite and marble: a guide to building stones in New Zealand. *Geological Society of New Zealand guidebook 8.* 57p.

Healy, J. 1992: Central volcanic region. *In* Soons, J.M.; Selby, M.J. (eds) Landforms of New Zealand 2nd Edition. Longman Paul, Auckland: 256-286.

Hewitt, A.E. 1992: New Zealand Soil Classification. *DSIR Land Resources scientific report 19*. 133p.

Hochstein, M.P.; Nixon, I.M. 1979: geophysical study of the Hauraki Depression, North Island, New Zealand. *New Zealand journal of geology and geophysics 22*: 1-19.

Hochstein, M.P.; Tearney, K.; Rawson, S.; Davidge, S.; Henrys, S.; Backshall, D. 1986: Structure of the Hauraki Rift (New Zealand). *Royal Society of New Zealand bulletin 24*: 333-348.

Hodder, A.P.W.; Green, B.E.; Lowe, D.J. 1990: A two-stage model for the formation of clay minerals from tephra-derived volcanic glass. *Clay minerals 25*: 313-327.

Houghton, B.F.; Wilson, C.J.N.; McWilliams, M.; Lanphere, M.A.; Weaver, S.D.; Briggs, R.M.; Pringle, M.S. 1994: Volcanic and structural evolution of a large silicic volcanic system: central Taupo Volcanic Zone, New Zealand. Submitted to *Geology*.

Hume, T.M.; Sherwood, A.M.; Nelson, C.S. 1975: Alluvial sedimentology of the Upper Pleistocene Hinuera Formation, Hamilton basin, New Zealand. *Journal of the Royal Society of New Zealand 5*: 421-462.

Kennedy, N.M. 1982: Tephric loess in Rotorua-Bay of Plenty region, North Island, New Zealand. *In* Wasson, R.J. (ed) Quaternary Dust Mantles of Australia, New Zealand and China. Australian National University, Canberra: 119-122.

Kennedy, N.M. 1988: Late Quaternary loess associated with the Mamaku Plateau, North Island, New Zealand. *In* Eden, D.N.; Furkert, R.J. (eds) Loess: Its Distribution, Geology and Soils. A.A. Balkema, Rotterdam: 71-80.

Kennedy, N.M. in press: New Zealand tephro-chronology as a tool in geomorphic history of c. 140 ka Mamaku Ignimbrite Plateau and in relating oxygen isotope stages. *Geomorphology 229*

Kennedy, N.M.; Pullar, W.A.; Pain, C.F. 1978: Late Quaternary land surfaces and geomorphic changes in the Rotorua Basin, North Island, New Zealand. *New Zealand journal of science 21*: 249-264.

Kimber, R.W.L.; Kennedy, N.M.; Milnes, A.R. in press: Amino acid racemization dating of a 140,000 year-old tephra-loess-palaeosol sequence on the Mamaku Plateau near Rotorua, New Zealand. *Australian journal of earth sciences*

Lowe, D.J. 1981: Origin and composite nature of late Quaternary air-fall deposits, Hamilton Basin, New Zealand. Unpiblished MSc thesis, University of Waikato, Hamilton.

Lowe, D.J. 1986: Controls on the rates of weathering and clay mineral genesis in airfall tephras: a review and New Zealand case study. *In* Colman, S.M.; Dethier, D.P. (eds) Rates of Chemical Weathering of Rocks and Minerals. Academic Press, Orlando: 265-330.

Lowe, D.J. 1988: Stratigraphy, age, composition, and correlation of late Quaternary tephras interbedded with organic sediments in Waikato lakes, North Island, New Zealand. *New Zealand journal of geology and geophysics 31*: 125-165.

Lowe, D.J.; Green, J.D. 1992: Lakes. *In* Soons, J.M.; Selby, M.J. (eds) Landforms of New Zealand 2nd Edition. Longman Paul, Auckland: 107-143.

Lowe, D.J.; Green, B.E. 1992a: A hydrofluoric acid dissolution method for determining volcanic glass content of tephra-derived soils (Andisols). *Australian journal of soil research 30*: 573-581.

McGlone, M.S. 1983: Holocene pollen diagrams, Lake Rotorua, North Island, New Zealand. *Journal of the Royal Society of New Zealand 13*: 53-65.

McGlone, M.S. 1988: New Zealand. *In* Huntley, B.; Webb, T.III (eds) Vegetational History. Kluwer Academic Publishers: 557-599.

McLeod, M. 1992: Soils of part northern Matamata County, North Island, New Zealand. *DSIR Land Resources scientific report 18*. 96p.

Murphy, R.P.; Seward, D. 1981: Stratigraphy, lithology, paleomagnetism, and fission track ages of some ignimbrite formations in the Matahana Basin, New Zealand. *New Zealand journal of geology and geophysics 24*: 325-331.

Nairn, I.A. 1989: Geological Map of New Zealand 1:50 000. Sheet V16C Mount Tarawera. New Zealand Geological Survey, Department of Scientific and Industrial Research, Wellington.

Nairn, I.A. 1992: The Te Rere and Okareka eruptive episodes — Okataina Volcanic Centre, Taupo Volcanic Zone, New Zealand. *New Zealand journal of geology and geophysics 35*: 93-108.

Nairn, I.A.; Wood, C.P. 1987: Acive volcanoes of Taupo Volcanic Zone. *New Zealand Geological Survey record 22*. 152p.

Newnham, R.M.; Lowe, D.J.; Green, J.D. 1989: Palynology, vegetation and climate of the Waikato lowlands, North Island, New Zealand, since c. 18,000 years ago. *Journal of the Royal Society of New Zealand 19*: 127-150.

Parfitt, R.L.; Pollock, J.A.; Furkert, R.J. (compilers) 1981: Guide book for Tour 1 Pre-conference North Island, New Zealand. *Soils With Variable Charge Conference,* Palmerston North, New Zealand. 153p.

Pillans, B.J.; McGlone, M.S.; Palmer, A.S.; Mildenhall, D.; Alloway, B.V.; Berger, G.W. 1993: The Last Glacial Maximum in central and southern North Island, New Zealand: a paleoenvironmental reconstruction using the Kawakawa Tephra Formation as a chronostratigraphic marker. *Palaeogeography, palaeoclimatology, palaeoecology 101*: 283-304.

Rijkse, W.C. 1979: Soils of Rotorua Lakes district, North Island, New Zealand. *New Zealand Soil survey report 43.* 124p.

Sase, T.; Hosono, M.; Utsugawa, T.; Aoki, K. 1988: Opal phytolith analysis of present and buried volcanic ash soils at Te Ngae Road tephra section, Rotorua Basin, North Island, New Zealand. *Quaternary research (Japan) 27*: 153-163.

Selby, M.J.; Lowe, D.J. 1992: The middle Waikato Basin and hills. *In* Soons, J.M.; Selby, M.J. (eds) Landforms of New Zealand 2nd Edition. Longman Paul, Auckland: 233-255.

Stokes, S.; Lowe, D.J.; Froggatt, P.C. 1992: Discriminant function analysis and correlation of late Quaternary rhyolitic tephra deposits from Taupo and Okataina volcanoes, New Zealand, using glass shard major element composition. *Quaternary international 13/14*: 103-117.

Vucetich, C.G.; Pullar, W.A. 1969: Stratigraphy and chronology of late Pleistocene volcanic ash beds in central North Island, New Zealand. *New Zealand journal of geology and geophysics 12*: 784-837.

Walker, G.P.L. 1983: Ignimbrite types and ignimbrite problems. *Journal of volcanology and geothermal research 17*: 65-88.

Walker, G.P.L.; Self, S.; Wilson, L. 1984: Tarawera 1886, New Zealand — a basaltic plinian fissure eruption. *Journal of volcanology and geothermal research 21*: 61-78.

Whitton, J.S.; Churchman, G.J. 1987: Standard methods for mineral analysis of soil survey samples for characterisation and classification in New Zealand Soil Bureau. *New Zealand Soil Bureau scientific report 79.*

Wilson, C.J.N. 1986. Reconnaissance stratigraphy and volcanology of ignimbrites from Mangakino Volcano. *Royal Society of New Zealand bulletin 23*: 179-193.

Wilson, C.J.N. 1993: Stratigraphy, chronology, styles and dynamics of late Quaternary erptions from Taupo volcano, New Zealand. *Philosophical transactions of the Royal Society, London A343*: 205-306.

Wilson, C.J.N.; Rogan, A.M.; Smith, I.E.M.; Northey, D.J.; Nairn, I.A.; Houghton, B.F. 1984: Caldera volcanoes of the Taupo Volcanic Zone, New Zealand. *Journal of geophysical research 89(B10)*: 8463-8484.

Wilson, C.J.N.; Houghton, B.F.; Lanphere, M.A.; Weaver, S.D. 1992: A new radiometric age estimate for the Rotoehu Ash from Mayor Island volcano, New Zealand. *New Zealand journal of geology and geophysics 35*: 371-374.